

Supporting Information

Mononuclear organogermanium(IV) catalysts for a [3+2] cycloaddition reaction

**Debayan Basu^a, Barshali Ghosh^a, Diship Srivastava^a, Niladri Patra^a and Hari Pada
Nayek^{a*}**

*^aDepartment of Chemistry and Chemical Biology, Indian Institute of Technology (Indian School
of Mines), Dhanbad-826004, Jharkhand, India*

Email: hpnayek@iitism.ac.in

Table of contents

Figure/Table	Content	Page
Figure S1	FT-IR spectra of Schiff base pro-ligand H₂L¹ and compound 1	4
Figure S2	FT-IR spectra of Schiff base pro-ligand H₂L² and compound 2	4
Figure S3	FT-IR spectra of Schiff base pro-ligand H₂L³ and compound 3	5
Figure S4	¹ H NMR (400 MHz, DMSO- <i>d</i> ₆) spectrum of compound 1	5
Figure S5	¹³ C{ ¹ H} NMR (100 MHz, DMSO- <i>d</i> ₆) spectrum of compound 1	6
Figure S6	¹ H NMR (400 MHz, DMSO- <i>d</i> ₆) spectrum of compound 2	6
Figure S7	¹³ C{ ¹ H} NMR (100 MHz, DMSO- <i>d</i> ₆) spectrum of compound 2	7
Figure S8	¹ H NMR (400 MHz, DMSO- <i>d</i> ₆) spectrum of compound 3	7
Figure S9	¹³ C{ ¹ H} NMR (100 MHz, DMSO- <i>d</i> ₆) spectrum of compound 3	8
Figure S10	HRMS (ESI) spectrum of compound 1	8
Figure S11	HRMS (ESI) spectrum of [M+H] ⁺ ion of compound 1	9
Figure S12	HRMS (ESI) spectrum of compound 2	9
Figure S13	HRMS (ESI) spectrum of [M+H] ⁺ ion of compound 2	10
Figure S14	HRMS (ESI) spectrum of compound 3	10
Figure S15	HRMS (ESI) spectrum of [M+H] ⁺ ion of compound 3	11
Table S1	Single crystal data collection and data refinement parameters for compound 1 and 2	12
Figure S16	Packing of 1 within the unit cell viewed along crystallographic <i>a</i> axis	13
Figure S17	Packing of 2 within the unit cell viewed along crystallographic <i>b</i> axis	13
Figure S18	Plot of % yield (isolated) of product vs. catalyst loading for the synthesis of 5-substituted 1 <i>H</i> -tetrazole between sodium azide and benzonitrile. Reaction conditions: benzonitrile (0.40 mmol), sodium azide (0.80 mmol), compound 1 (2-10 mol %). Time: 8 h at 100 °C.	14
Figure S19	Plot of % yield (isolated) of product vs. time for the synthesis of 5-substituted 1 <i>H</i> -tetrazole between sodium azide and benzonitrile. Reaction conditions: benzonitrile (0.40 mmol), sodium azide (0.80 mmol), compound 1 (6 mol %) at 100 °C.	14
Table S2	Isolated yields of 5-substituted 1 <i>H</i> -tetrazoles of various nitriles with sodium azide	15
Table S3	Characterization of isolated 5-substituted 1 <i>H</i> -tetrazoles of various nitriles with sodium azide	16
Figure S20	¹ H NMR (400 MHz, DMSO- <i>d</i> ₆) spectrum of 4a	17
Figure S21	¹³ C{ ¹ H} NMR (100 MHz, DMSO- <i>d</i> ₆) spectrum of 4a	18
Figure S22	¹ H NMR (400 MHz, DMSO- <i>d</i> ₆) spectrum of 4b	18
Figure S23	¹³ C{ ¹ H} NMR (100 MHz, DMSO- <i>d</i> ₆) spectrum of 4b	19
Figure S24	¹ H NMR (400 MHz, CDCl ₃) spectrum of 4c	19
Figure S25	¹³ C{ ¹ H} NMR (100 MHz, CDCl ₃) spectrum of 4c	20
Figure S26	¹ H NMR (400 MHz, DMSO- <i>d</i> ₆) spectrum of 4d	20
Figure S27	¹³ C{ ¹ H} NMR (100 MHz, DMSO- <i>d</i> ₆) spectrum of 4d	21
Figure S28	¹ H NMR (400 MHz, DMSO- <i>d</i> ₆) spectrum of 4e	21
Figure S29	¹³ C{ ¹ H} NMR (100 MHz, DMSO- <i>d</i> ₆) spectrum of 4e	22
Figure S30	¹ H NMR (400 MHz, CDCl ₃) spectrum of 4f	22
Figure S31	¹³ C{ ¹ H} NMR (100 MHz, CDCl ₃) spectrum of 4f	23
Figure S32	¹ H NMR (400 MHz, DMSO- <i>d</i> ₆) spectrum of 4g	23
Figure S33	¹³ C{ ¹ H} NMR (100 MHz, DMSO- <i>d</i> ₆) spectrum of 4g	24
Figure S34	¹ H NMR (400 MHz, DMSO- <i>d</i> ₆) spectrum of 4h	24

Figure S35	$^{13}\text{C}\{^1\text{H}\}$ NMR (100 MHz, DMSO- d_6) spectrum of 4h	25
Figure S36	^1H NMR (400 MHz, DMSO- d_6) spectrum of 4i	25
Figure S37	$^{13}\text{C}\{^1\text{H}\}$ NMR (100 MHz, DMSO- d_6) spectrum of 4i	26
Figure S38	^1H NMR (400 MHz, DMSO- d_6) spectrum of 4j	26
Figure S39	$^{13}\text{C}\{^1\text{H}\}$ NMR (100 MHz, DMSO- d_6) spectrum of 4j	27
Figure S40	^1H NMR (400 MHz, DMSO- d_6) spectrum of 4k	27
Figure S41	$^{13}\text{C}\{^1\text{H}\}$ NMR (100 MHz, DMSO- d_6) spectrum of 4k	28
Figure S42	^1H NMR (400 MHz, DMSO- d_6) spectrum of 4l	28
Figure S43	$^{13}\text{C}\{^1\text{H}\}$ NMR (100 MHz, DMSO- d_6) spectrum of 4l	29
Figure S44	1,5-disubstituted intermediate (B) and 2,5-disubstituted Intermediate (B') with numbering scheme in Path I and Path II	30
Table S4	Bond lengths present in various stationary states. All values are reported in Å	30
Figure S45	DFT-optimized geometry of azide ion	31
Table S5	Cartesian coordinates of DFT-optimized geometry of azide ion	31
Figure S46	DFT-optimized geometry of benzonitrile	32
Table S6	Cartesian coordinates of DFT-optimized geometry of benzonitrile.	32
Figure S47	DFT-optimized geometry of compound 1 [Ge(IV) compound]	33
Table S7	Cartesian coordinates of DFT-optimized geometry of compound 1 [Ge(IV) compound]	33
Figure S48	DFT-optimized geometry of compound 1 and azide (Transition state 1)	35
Table S8	Cartesian coordinates of DFT-optimized geometry of compound 1 and azide (Transition state 1)	35
Figure S49	DFT-optimized geometry of compound 1 and azide (Intermediate A)	37
Table S9	Cartesian coordinates of DFT-optimized geometry of compound 1 and azide (Intermediate A)	37
Figure S50	DFT-optimized geometry of Intermediate A and benzonitrile (Transition state 2)	39
Table S10	Cartesian coordinates of DFT-optimized geometry of Intermediate A and benzonitrile (Transition state 2)	40
Figure S51	DFT-optimized geometry of Intermediate A and benzonitrile (Transition state 2')	42
Table S11	Cartesian coordinates of DFT-optimized geometry of Intermediate A and benzonitrile (Transition state 2')	42
Figure S52	DFT-optimized geometry of Intermediate A and benzonitrile (Intermediate B)	45
Table S12	Cartesian coordinates of DFT-optimized geometry of Intermediate A and benzonitrile (Intermediate B)	45
Figure S53	DFT-optimized geometry of Intermediate A and benzonitrile (Intermediate B')	48
Table S13	Cartesian coordinates of DFT-optimized geometry of Intermediate A and benzonitrile (Intermediate B')	48
Figure S54	DFT-optimized geometry of 5-substituted 1 <i>H</i> -tetrazole	51
Table S14	Cartesian coordinates of DFT-optimized geometry of 5-substituted 1 <i>H</i> -tetrazole	51
Table S15	Different catalysts used for the synthesis of 5-substituted 1 <i>H</i> -tetrazoles.	52

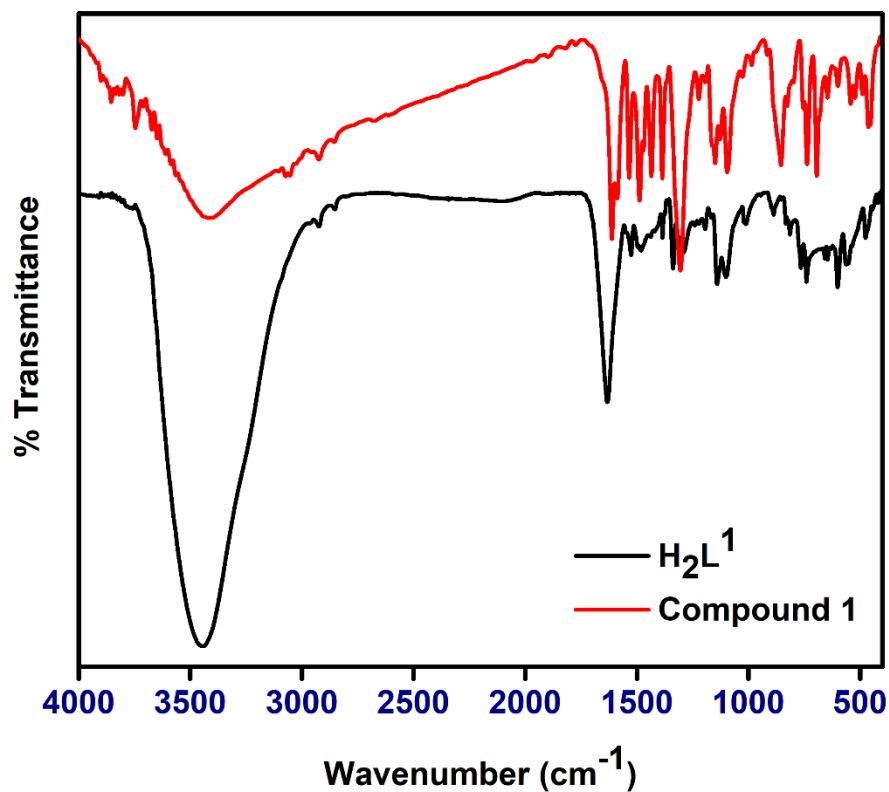


Figure S1. FT-IR spectra of Schiff base pro-ligand H_2L^1 and compound 1.

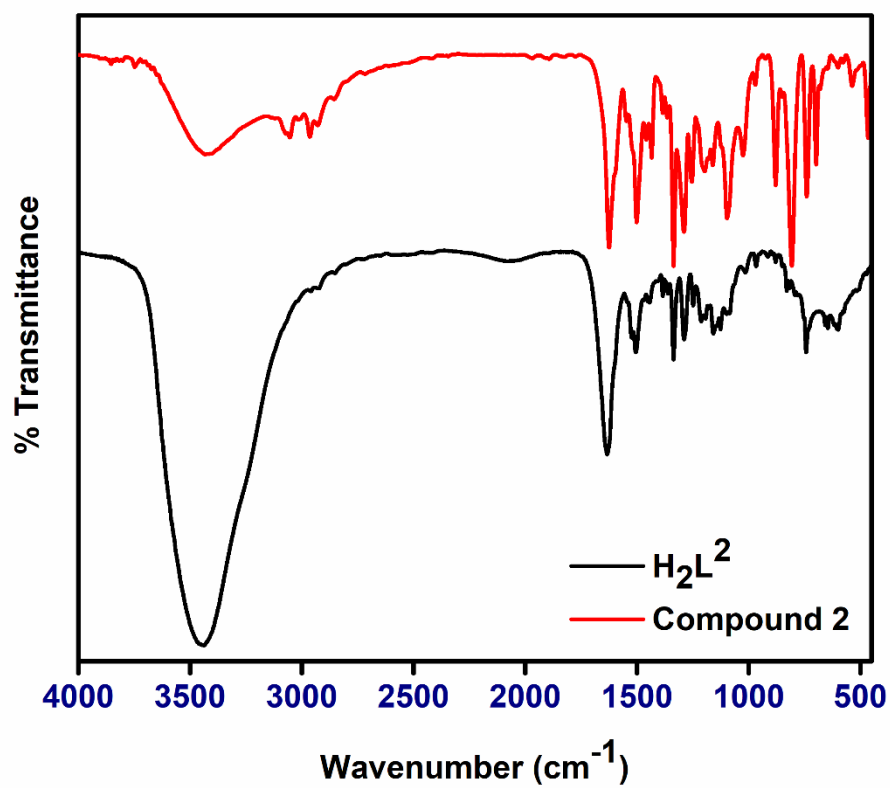


Figure S2. FT-IR spectra of Schiff base pro-ligand H_2L^2 and compound 2.

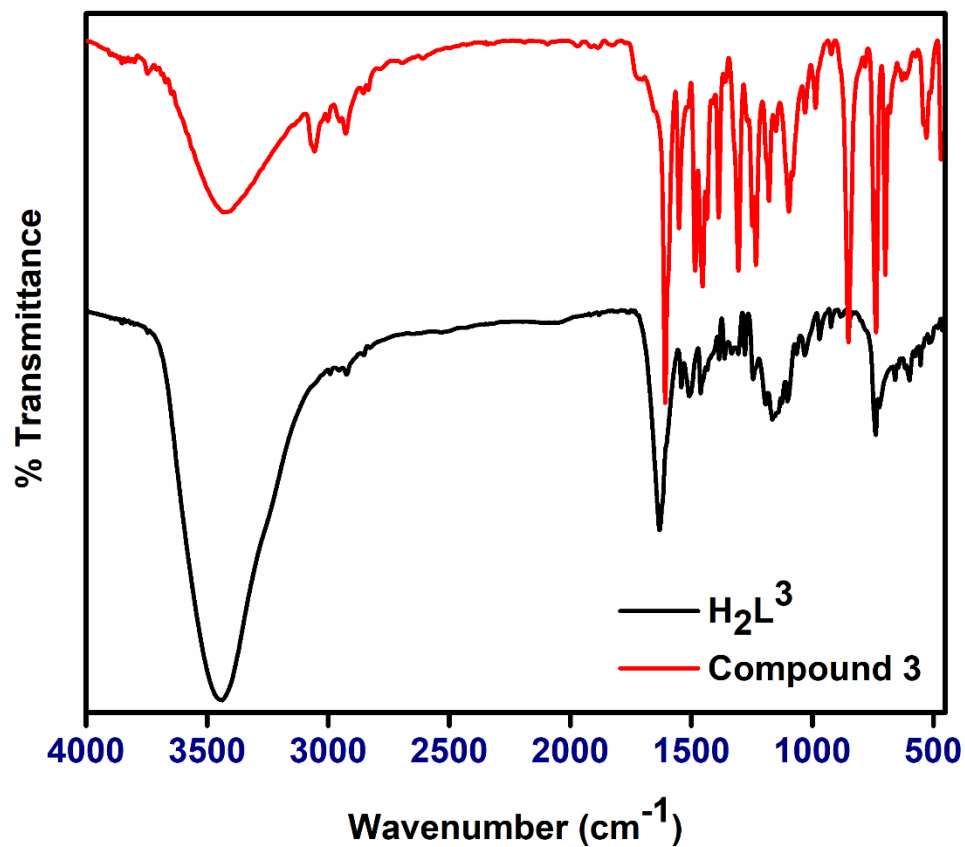


Figure S3. FT-IR spectra of Schiff base pro-ligand H_2L^3 and compound 3.

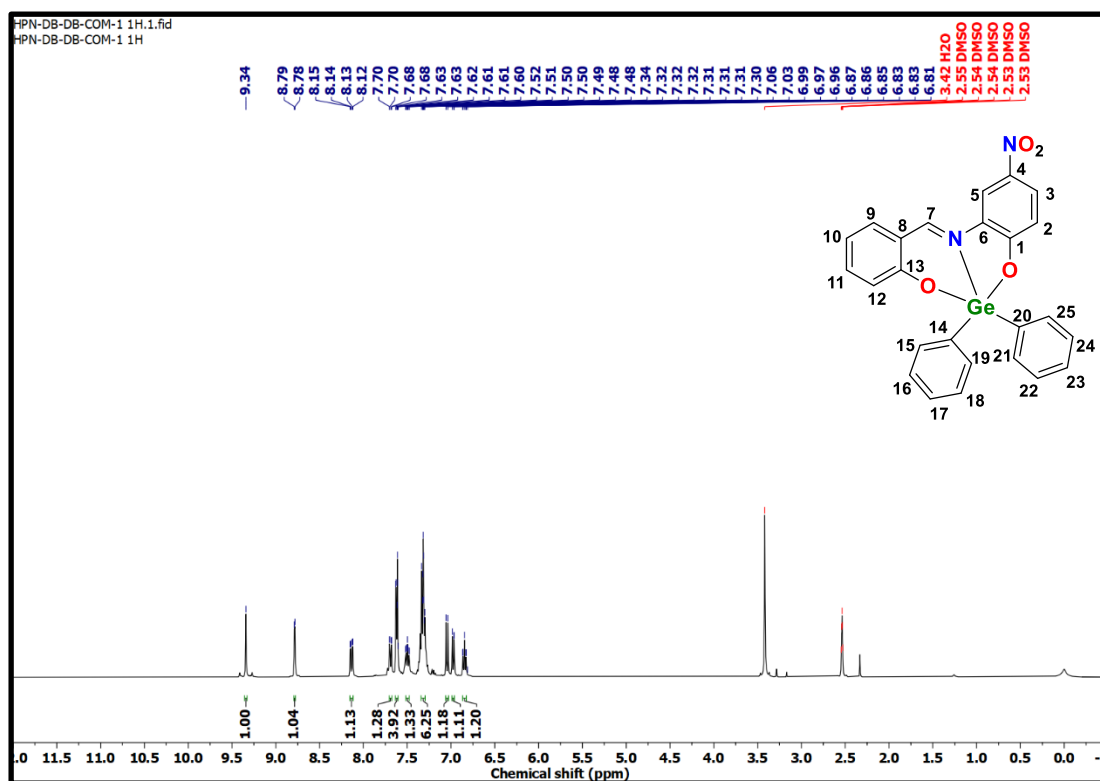


Figure S4. 1H NMR (400 MHz, $DMSO-d_6$) spectrum of compound 1.

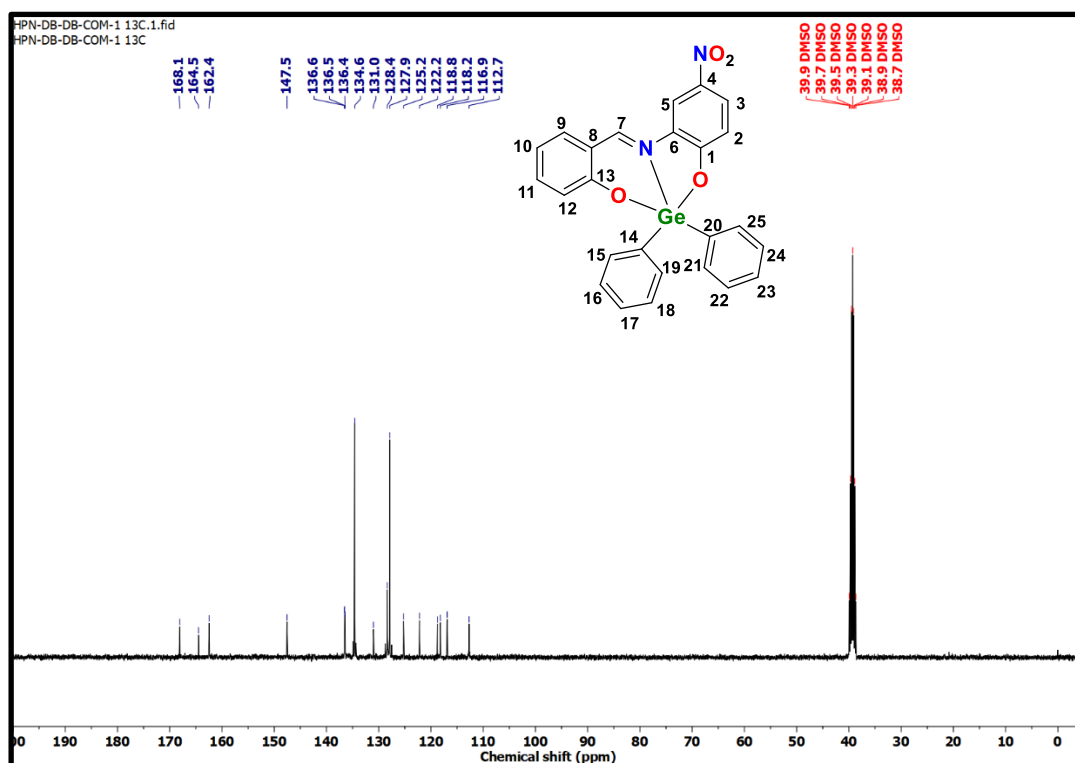


Figure S5. $^{13}\text{C}\{^1\text{H}\}$ NMR (100 MHz, $\text{DMSO-}d_6$) spectrum of compound 1.

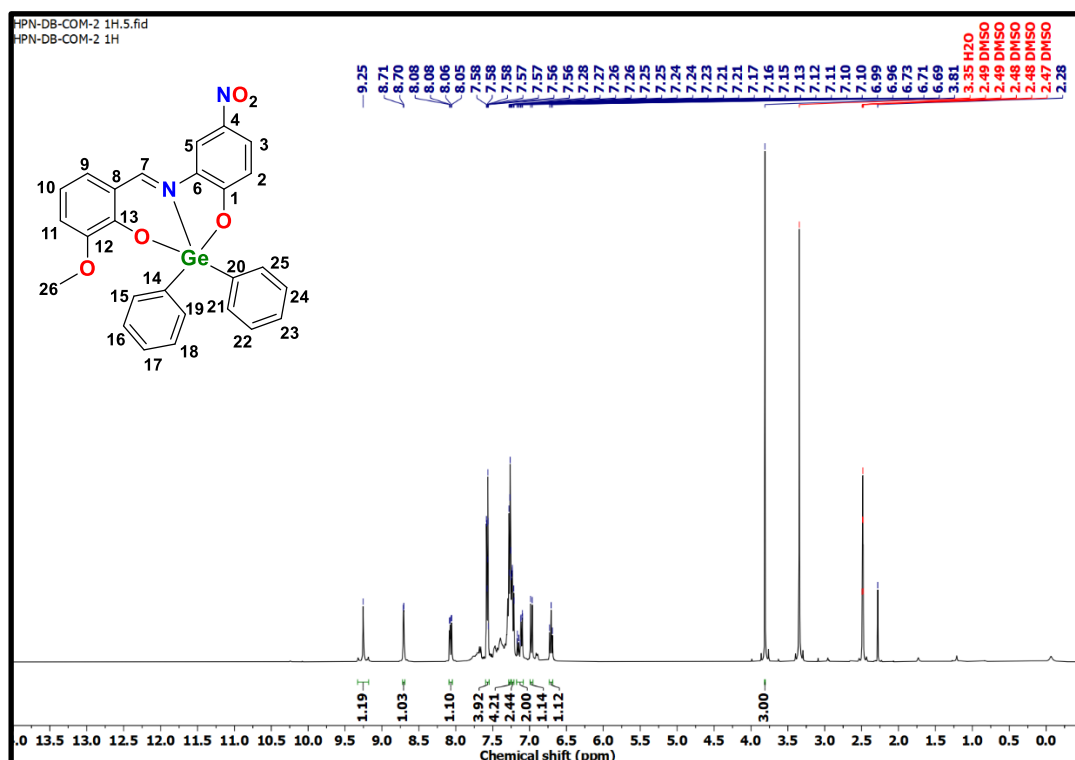


Figure S6. ^1H NMR (400 MHz, $\text{DMSO-}d_6$) spectrum of compound 2.

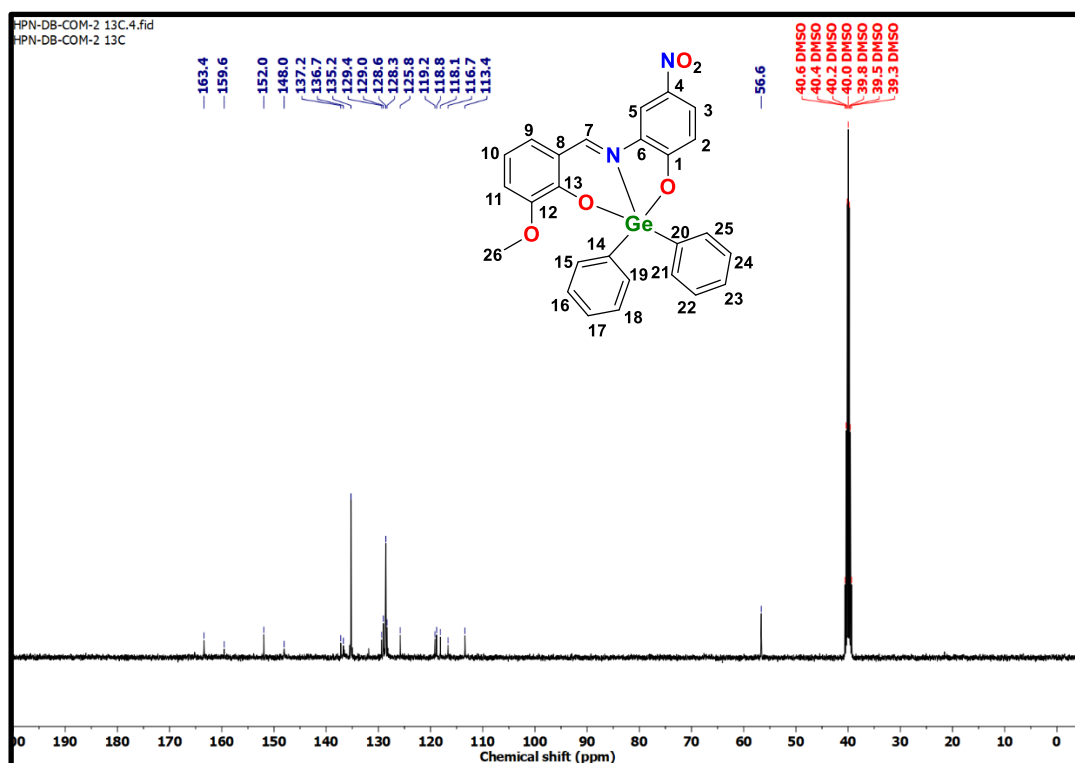


Figure S7. $^{13}\text{C}\{^1\text{H}\}$ NMR (100 MHz, $\text{DMSO-}d_6$) spectrum of compound 2.

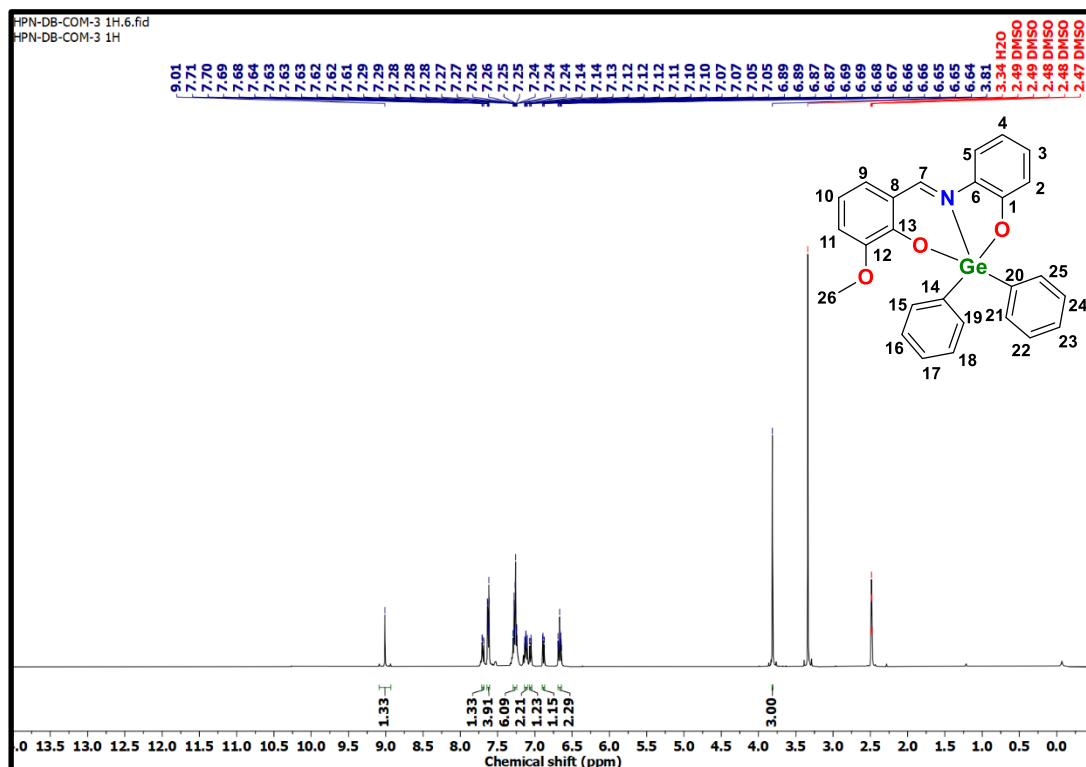


Figure S8. ^1H NMR (400 MHz, $\text{DMSO-}d_6$) spectrum of compound 3.

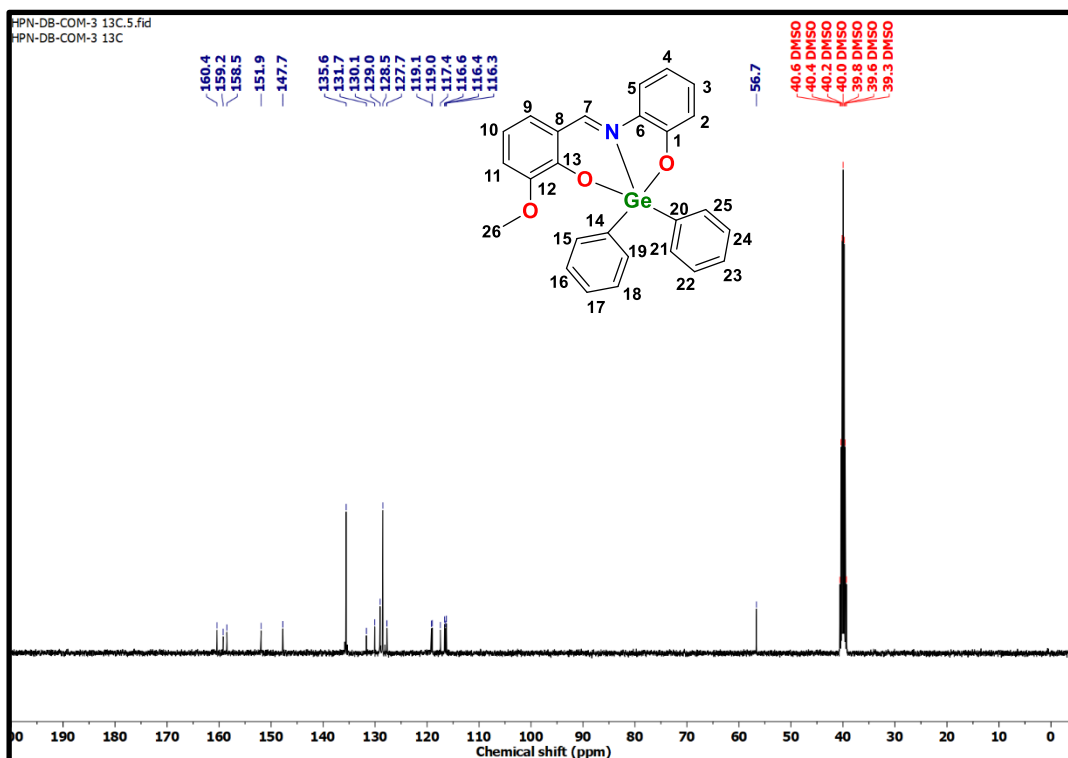


Figure S9. $^{13}\text{C}\{^1\text{H}\}$ NMR (100 MHz, $\text{DMSO-}d_6$) spectrum of compound 3.

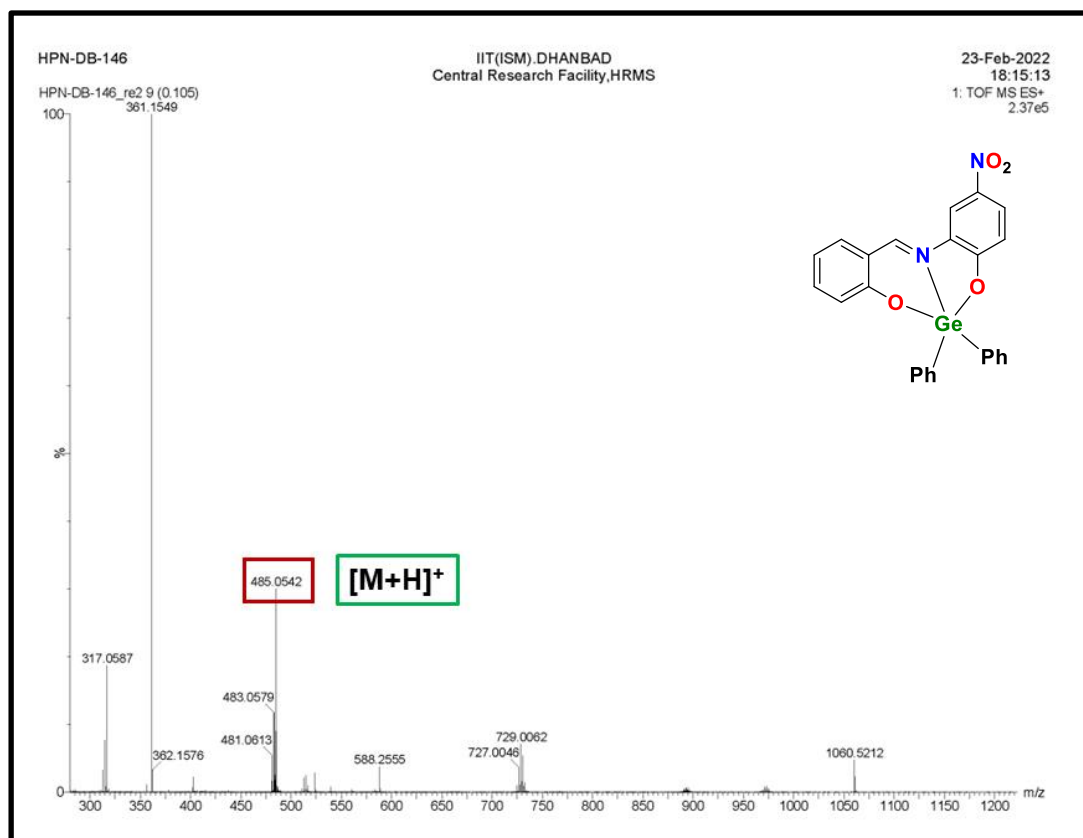


Figure S10. HRMS (ESI) spectrum of compound 1.

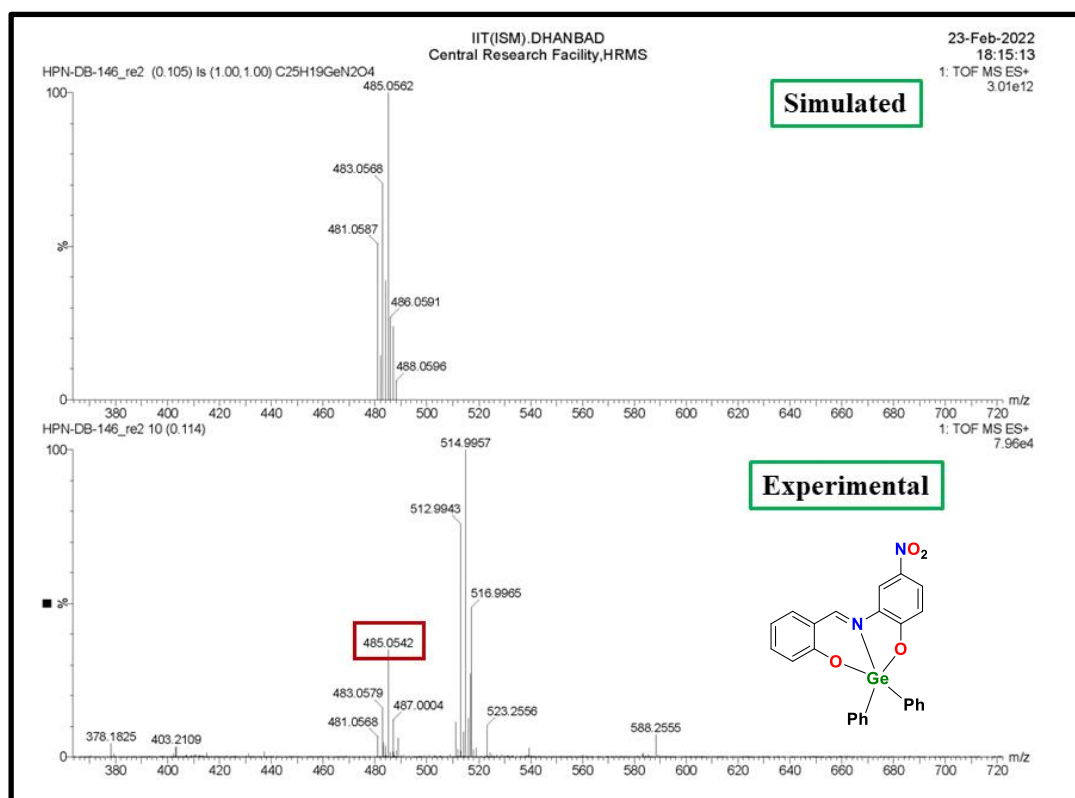


Figure S11. HRMS (ESI) spectrum of $[M+H]^+$ ion of compound 1.

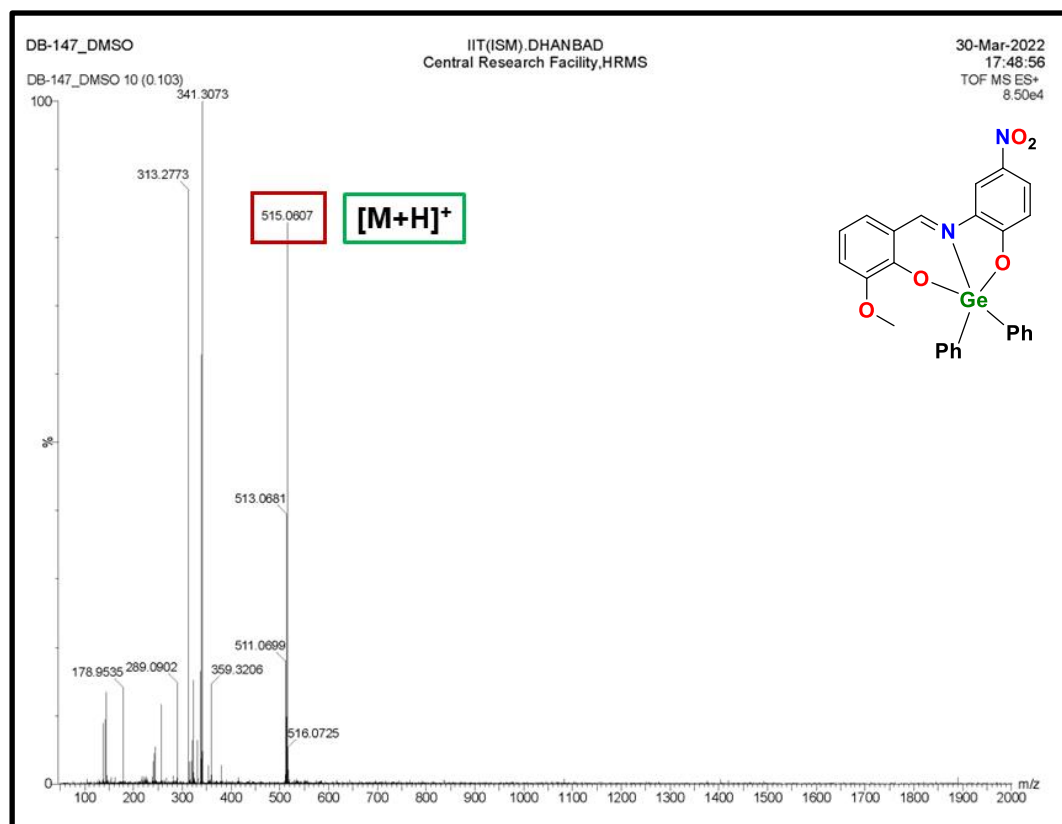


Figure S12. HRMS (ESI) spectrum of compound 2.

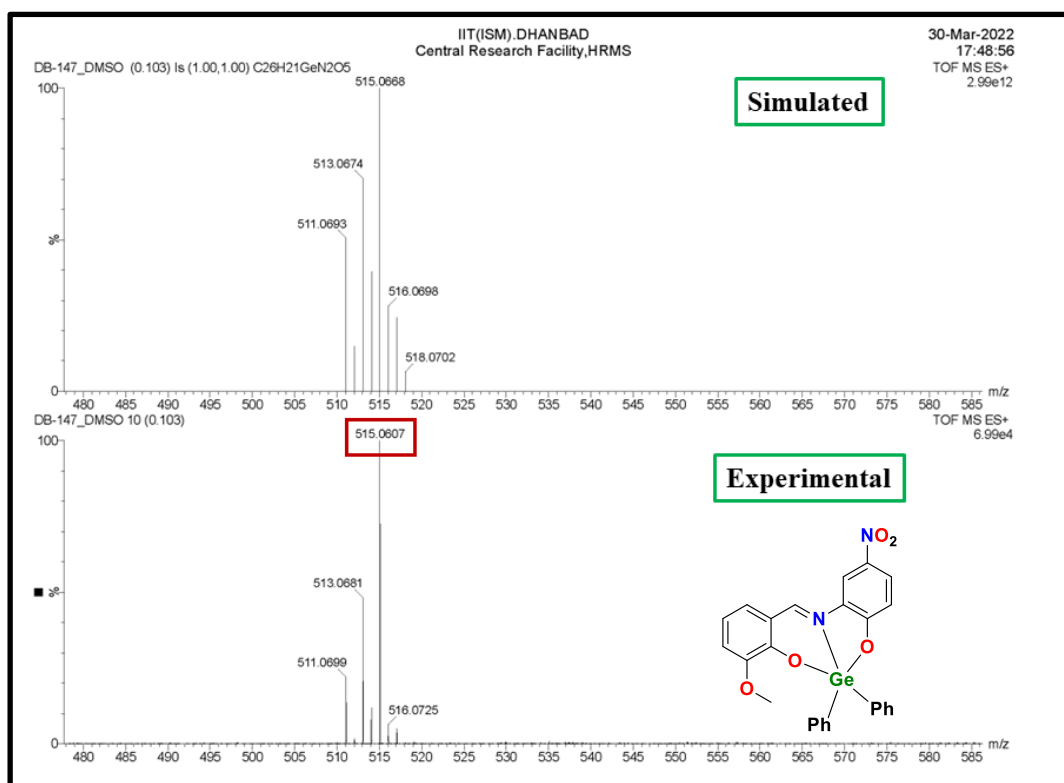


Figure S13. HRMS (ESI) spectrum of $[M+H]^+$ ion of compound 2.

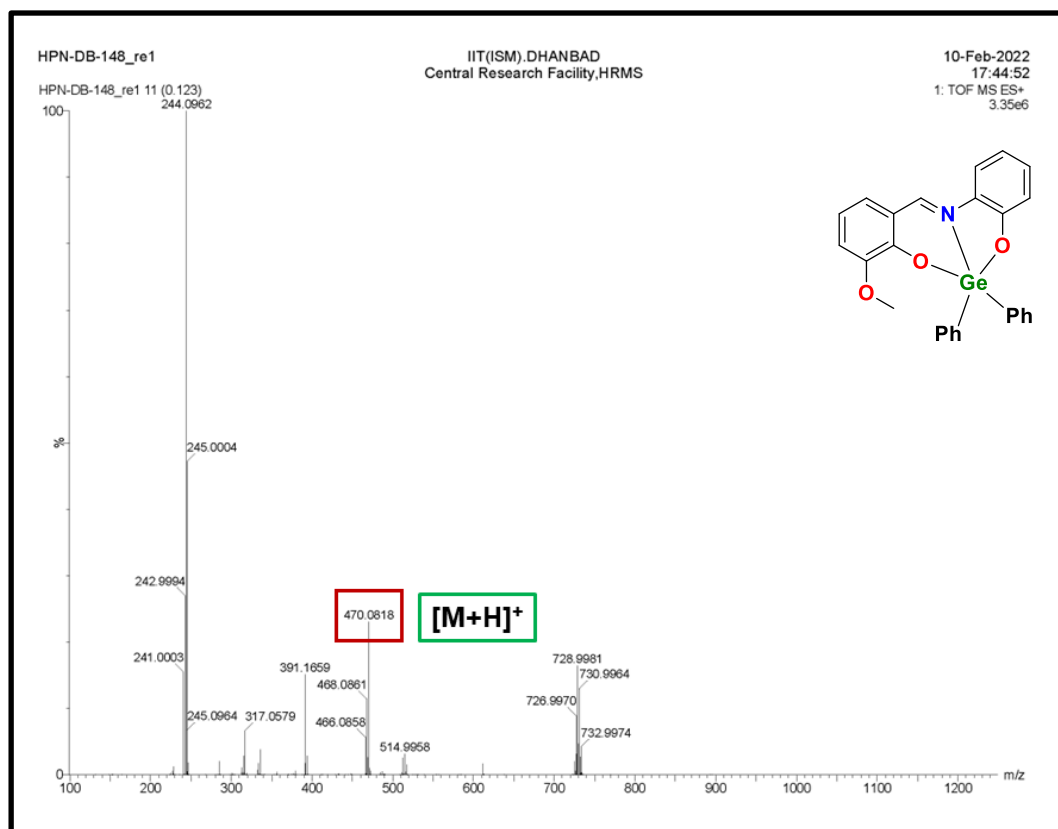


Figure S14. HRMS (ESI) spectrum of compound 3.

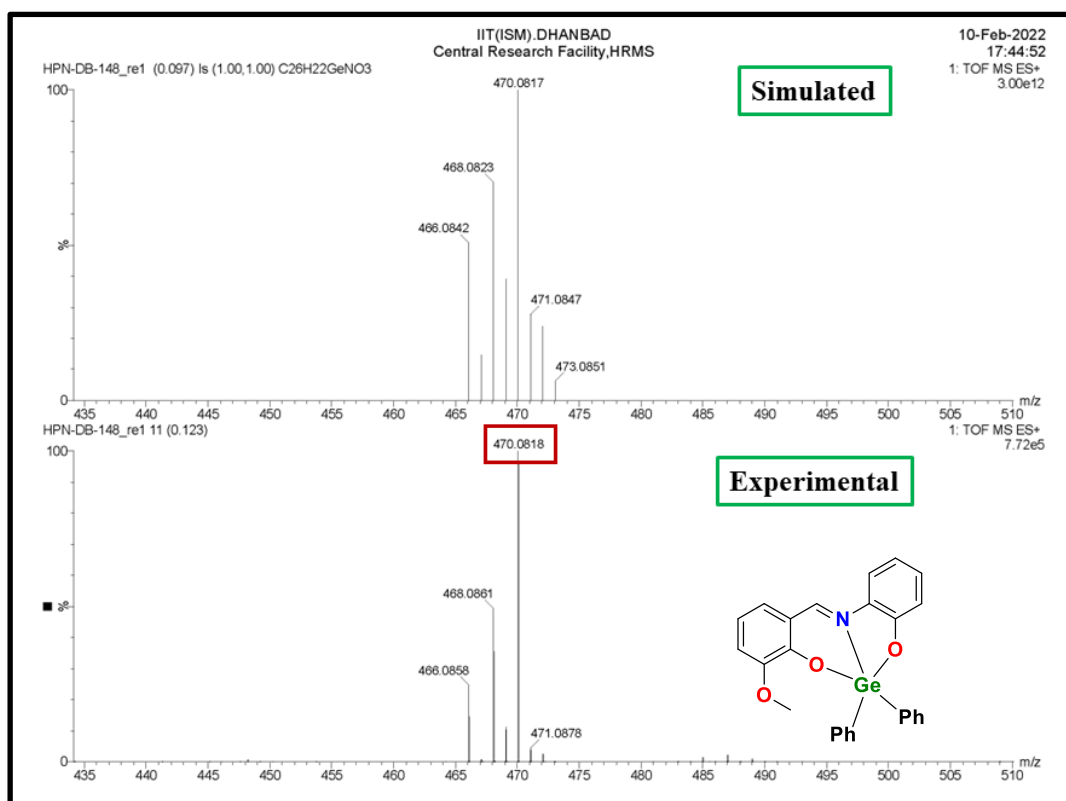


Figure S15. HRMS (ESI) spectrum of $[M+H]^+$ ion of compound **3**.

X-ray crystallography:

The crystallographic data of **1-2** were collected on a Rigaku SuperNova diffractometer equipped with an Eos S2 CCD detector, using Mo-K α radiation with graphite monochromator ($\lambda = 0.71073 \text{ \AA}$) at $T = 293(2) \text{ K}$. The structure was solved with the ShelXT 2014/5 (Sheldrick, 2014) solution program and by using Olex2 as the graphical interface. The model was refined with version 2018/3 of XL using Least Squares minimization. Non-hydrogen atoms were anisotropically refined. H-atoms were included in the refinement of calculated positions riding on their carrier atoms. The function minimized was $[\sum w(F_o^2 - F_c^2)^2]$ ($w = 1 / [\sigma^2(F_o^2) + (aP)^2 + bP]$), where $P = (\text{Max}(F_o^2, 0) + 2F_c^2) / 3$ with $\sigma^2(F_o^2)$ from counting statistics. The function $R1$ and $wR2$ were $(\sum ||F_o| - |F_c||) / \sum |F_o|$ and $[\sum w(F_o^2 - F_c^2)^2 / \sum wF_o^4]^{1/2}$, respectively. CCDC 2328314-2328315 contain the supplementary crystallographic data for compounds **1-2**. These data can be obtained free of charge from The Cambridge Crystallographic Data Centre via www.ccdc.cam.ac.uk/data_request/cif

Table S1. Single crystal data collection and data refinement parameters for compound **1** and **2**.

Compound	1	2
Empirical formula	C ₂₅ H ₁₈ GeN ₂ O ₄	C ₂₆ H ₂₀ GeN ₂ O ₅
Formula weight	483.00	513.03
Temperature/K	293(2)	293(2)
Crystal system	triclinic	triclinic
Space group	<i>P</i> -1	<i>P</i> -1
<i>a</i> /Å	7.9042(8)	11.1870(5)
<i>b</i> /Å	9.6253(9)	12.4501(6)
<i>c</i> /Å	14.8290(13)	16.3530(8)
α /°	78.913(7)	81.627(4)
β /°	89.952(8)	89.040(4)
γ /°	73.801(8)	82.921(4)
Volume/Å ³	1061.51(2)	2236.18(19)
<i>Z</i>	2	4
$\rho_{\text{calc}}/\text{cm}^3$	1.511	1.524
μ/mm^{-1}	1.479	1.412
<i>F</i> (000)	492.0	1048.0
Crystal size/mm ³	0.13 × 0.12 × 0.10	0.12 × 0.10 × 0.08
Radiation	MoK α (λ = 0.71073)	MoK α (λ = 0.71073)
2 θ range for data collection/°	4.498 to 53.998	3.874 to 52.744
Index ranges	-10 ≤ <i>h</i> ≤ 10, -12 ≤ <i>k</i> ≤ 12, -18 ≤ <i>l</i> ≤ 18	-13 ≤ <i>h</i> ≤ 13, -15 ≤ <i>k</i> ≤ 15, -20 ≤ <i>l</i> ≤ 20
Reflections collected	16290	19042
Independent reflections	4609 [R _{int} = 0.0774, R _{sigma} = 0.0690]	9148 [R _{int} = 0.0404, R _{sigma} = 0.0694]
Data/reIntermediateaints/parameters	4609/0/289	9148/0/615
Goodness-of-fit on F ²	1.053	0.936
Final R indexes [<i>I</i> ≥ 2 σ (<i>I</i>)]	R ₁ = 0.0535, wR ₂ = 0.1420	R ₁ = 0.0418, wR ₂ = 0.0741
Final R indexes [all data]	R ₁ = 0.0752, wR ₂ = 0.1522	R ₁ = 0.0830, wR ₂ = 0.0825
Largest diff. peak/hole / e Å ⁻³	1.05/-0.68	0.35/-0.33

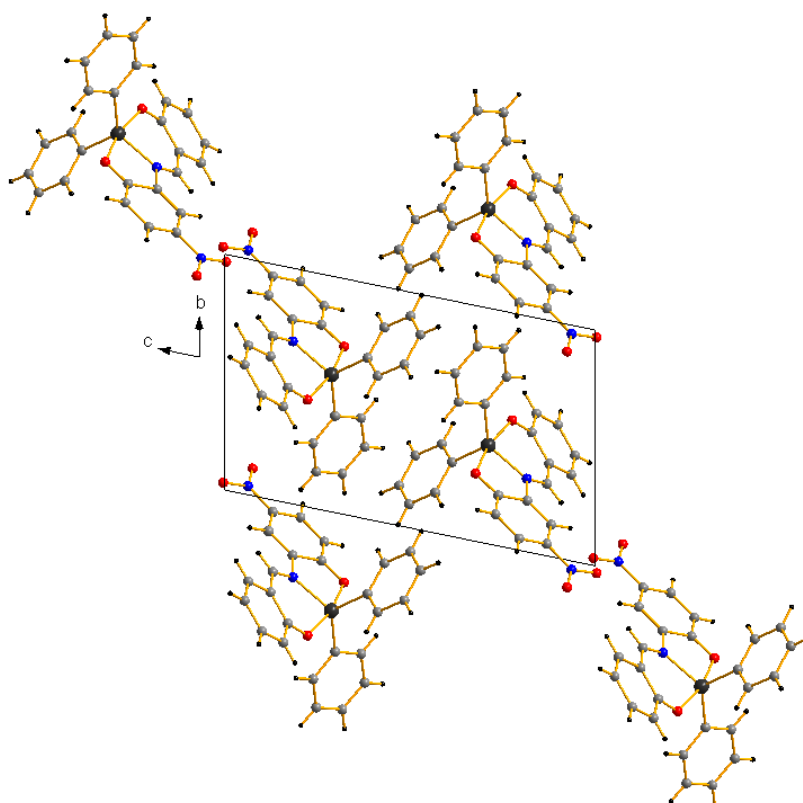


Figure S16. Packing of **1** within the unit cell viewed along crystallographic *a* axis.

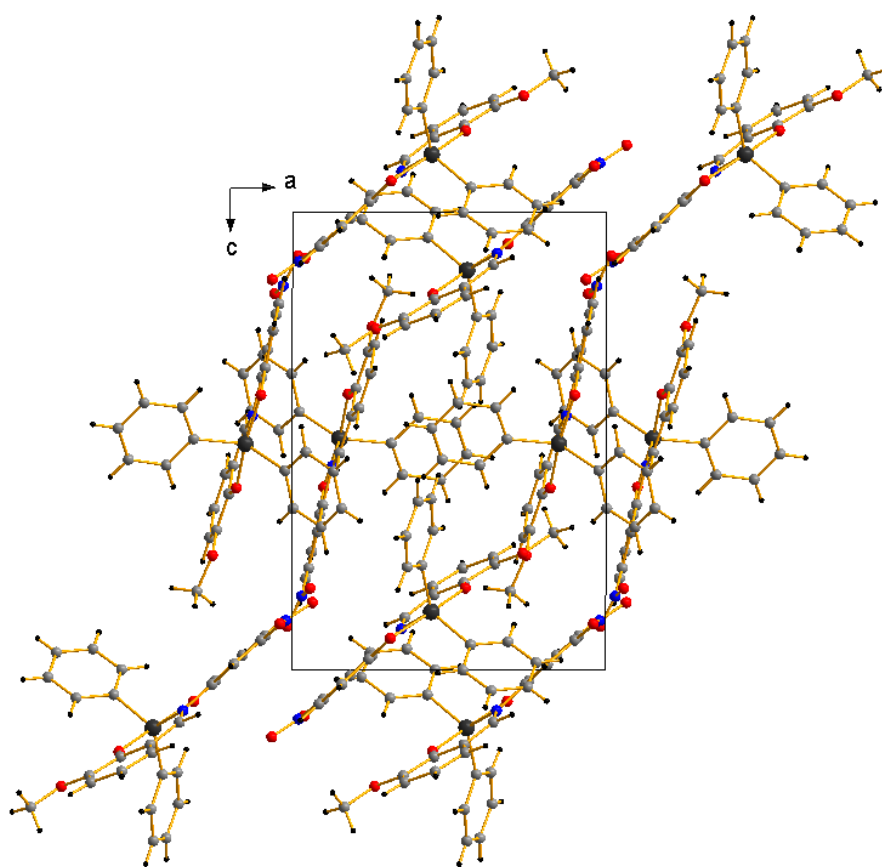


Figure S17. Packing of **2** within the unit cell viewed along crystallographic *b* axis.

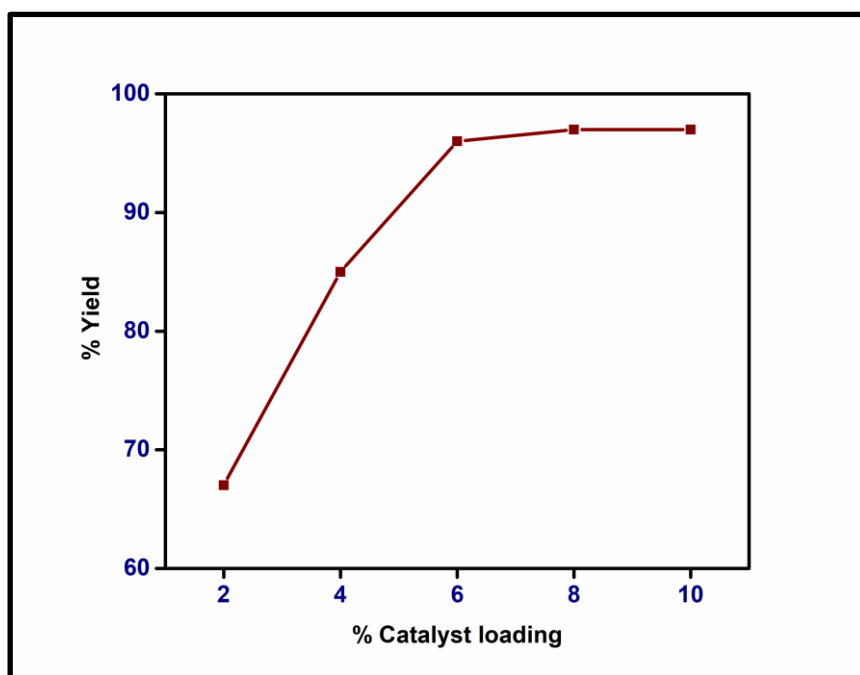


Figure S18. Plot of % yield (isolated) of product vs. catalyst loading for the synthesis of 5-substituted 1*H*-tetrazole between sodium azide and benzonitrile. Reaction condition: benzonitrile (0.40 mmol), sodium azide (0.80 mmol), compound **1** (2-10 mol %). Time: 8 h at 100 °C.

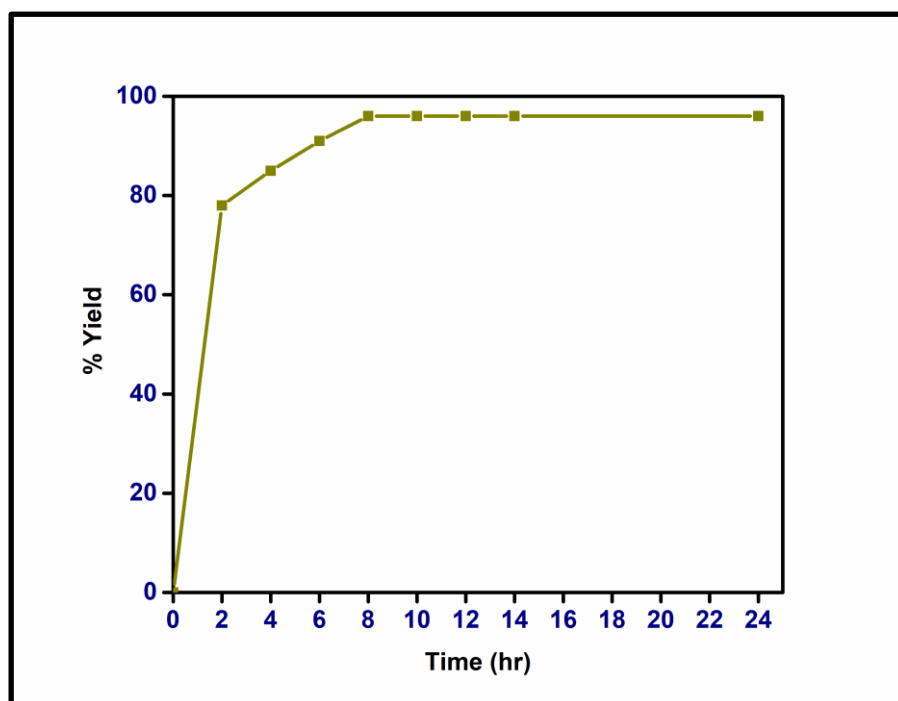
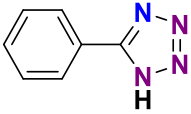
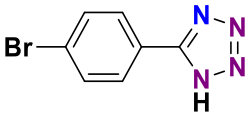
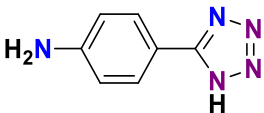
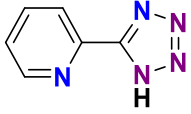
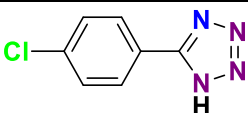
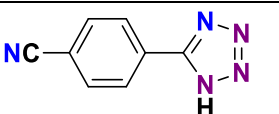
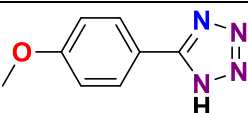
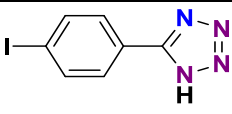
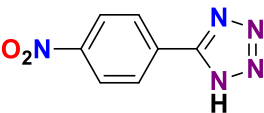


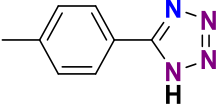
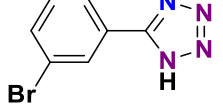
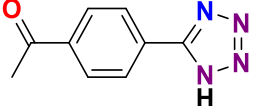
Figure S19. Plot of % yield (isolated) of product vs. time for the synthesis of 5-substituted 1*H*-tetrazole between sodium azide and benzonitrile. Reaction condition: benzonitrile (0.40 mmol), sodium azide (0.80 mmol), compound **1** (6 mol %) at 100 °C.

Table S2. Isolated yields of 5-substituted 1*H*-tetrazoles of various nitriles with sodium azide.

$\text{RCN} + \text{NaN}_3 \xrightarrow[\text{Solvent-free, 100 } ^\circ\text{C, 8h}]{\text{Catalyst (6 mol\%)}} \text{R}-\text{C}(\text{N}=\text{N}-\text{N}=\text{N})-\text{NH}$						
Entry	Nitriles	Product	Code	Yield (%)	TON	TOF (h ⁻¹)
1			4a	96	16	2
2			4b	94	15.7	1.9
3			4c	76	12.7	1.6
4			4d	91	15.2	1.9
5			4e	92	15.3	1.9
6			4f	84	14	1.8
7			4g	88	14.7	1.8
8			4h	89	14.8	1.9
9			4i	94	15.7	2
10			4j	90	15	1.9
11			4k	83	13.8	1.7
12			4l	93	15.5	1.9

Table S3. Characterization of isolated 5-substituted 1*H*-tetrazoles of various nitriles with sodium azide.

 <p>5-phenyl-1<i>H</i>-tetrazole</p>	<p>4a¹: Off-white solid. ¹H NMR (400 MHz, DMSO-<i>d</i>₆) δ 8.04 – 8.00 (m, 2H), 7.62 – 7.57 (m, 3H). ¹³C{¹H} NMR (100 MHz, DMSO-<i>d</i>₆) δ 155.8, 131.8, 129.9, 127.4, 124.6.</p>
 <p>5-(4-bromophenyl)-1<i>H</i>-tetrazole</p>	<p>4b²: Off-white solid. ¹H NMR (400 MHz, DMSO-<i>d</i>₆) δ 7.98 – 7.94 (m, 2H), 7.83 – 7.79 (m, 2H). ¹³C{¹H} NMR (100 MHz, DMSO-<i>d</i>₆) δ 155.5, 133.0, 129.4, 125.2, 124.0.</p>
 <p>4-(1<i>H</i>-tetrazol-5-yl)aniline</p>	<p>4c¹: Light yellow solid. ¹H NMR (400 MHz, CDCl₃) δ 7.41 – 7.37 (m, 2H), 6.66 – 6.62 (m, 2H), 4.21 (s, 2H, –NH₂). ¹³C{¹H} NMR (100 MHz, CDCl₃) δ 150.5, 133.8, 120.2, 114.5, 100.0.</p>
 <p>2-(1<i>H</i>-tetrazol-5-yl)pyridine</p>	<p>4d¹: Light solid. ¹H NMR (400 MHz, DMSO-<i>d</i>₆) δ 8.74 (m, 1H), 8.20 – 8.16 (m, 1H), 8.02 (m, 1H), 7.57 (m, 1H). ¹³C{¹H} NMR (100 MHz, DMSO-<i>d</i>₆) δ 155.3, 150.5, 144.1, 138.6, 126.5, 123.0.</p>
 <p>5-(4-chlorophenyl)-1<i>H</i>-tetrazole</p>	<p>4e¹: Off-white solid. ¹H NMR (400 MHz, DMSO-<i>d</i>₆) δ 8.06 – 7.99 (m, 2H), 7.71 – 7.62 (m, 2H). ¹³C{¹H} NMR (100 MHz, DMSO-<i>d</i>₆) δ 155.3, 136.4, 130.0, 129.2, 123.7.</p>
 <p>5-(<i>p</i>-tolyl)-1<i>H</i>-tetrazole</p>	<p>4f³: White solid. ¹H NMR (400 MHz, DMSO-<i>d</i>₆) δ 8.18 (d, <i>J</i> = 8.0 Hz, 2H), 8.05 (d, <i>J</i> = 8.0 Hz, 2H). ¹³C{¹H} (100 MHz, DMSO-<i>d</i>₆) δ 155.8, 133.8, 129.3, 128.1, 118.7, 113.9.</p>
 <p>5-(4-methoxyphenyl)-1<i>H</i>-tetrazole</p>	<p>4g⁴: Light yellow solid. ¹H NMR (400 MHz, DMSO-<i>d</i>₆) δ 7.98 – 7.94 (m, 2H), 7.16 – 7.12 (m, 2H), 3.82 (s, 3H, –OCH₃). ¹³C{¹H} NMR (100 MHz, DMSO-<i>d</i>₆) δ 162.0, 155.4, 129.2, 116.1, 115.4, 55.8.</p>
 <p>5-(4-iodophenyl)-1<i>H</i>-tetrazole</p>	<p>4h⁵: Light brown solid. ¹H NMR (400 MHz, DMSO-<i>d</i>₆) δ 7.97 (d, <i>J</i> = 8.2 Hz, 2H), 7.79 (d, <i>J</i> = 8.3 Hz, 2H). ¹³C{¹H} NMR (100 MHz, DMSO-<i>d</i>₆) δ 138.8, 129.2, 124.2, 120.6, 98.9.</p>
 <p>5-(4-nitrophenyl)-1<i>H</i>-tetrazole</p>	<p>4i¹: Off-white solid. ¹H NMR (400 MHz, DMSO-<i>d</i>₆) δ 8.04 – 7.98 (m, 2H), 7.66 – 7.60 (m, 2H). ¹³C{¹H} NMR (100 MHz, DMSO-<i>d</i>₆) δ 136.2, 130.0, 129.1, 124.1.</p>

 <p>5-(<i>p</i>-tolyl)-1<i>H</i>-tetrazole</p>	<p>4j⁴: Light yellow solid. ¹H NMR (400 MHz, DMSO-<i>d</i>₆) δ 7.91 (d, <i>J</i> = 7.9 Hz, 2H), 7.40 (d, <i>J</i> = 7.9 Hz, 2H), 2.37 (s, 3H, -CH₃). ¹³C{¹H} NMR (100 MHz, DMSO-<i>d</i>₆) δ 155.0, 141.1, 129.9, 126.8, 121.2, 20.9.</p>
 <p>5-(3-bromophenyl)-1<i>H</i>-tetrazole</p>	<p>4k³: White solid. ¹H NMR (400 MHz, DMSO-<i>d</i>₆) δ 8.18 (t, <i>J</i> = 1.8 Hz, 1H), 8.02 (dt, <i>J</i> = 7.8, 1.3 Hz, 1H), 7.76 (m, 1.0 Hz, 1H), 7.54 (t, <i>J</i> = 7.9 Hz, 1H). ¹³C{¹H} NMR (100 MHz, DMSO-<i>d</i>₆) δ 155.2, 134.3, 132.1, 129.8, 127.2, 126.4, 122.9.</p>
 <p>1-(4-(1<i>H</i>-tetrazol-5-yl)phenyl)ethan-1-one</p>	<p>4l³: Light yellow solid. ¹H NMR (400 MHz, DMSO-<i>d</i>₆) δ 8.15 (d, <i>J</i> = 8.5 Hz, 2H), 8.12 (d, <i>J</i> = 8.6 Hz, 2H), 2.61 (s, 3H, -CH₃). ¹³C{¹H} NMR (100 MHz, DMSO-<i>d</i>₆) δ 197.9, 162.8, 138.9, 129.6, 128.8, 127.7, 27.3.</p>

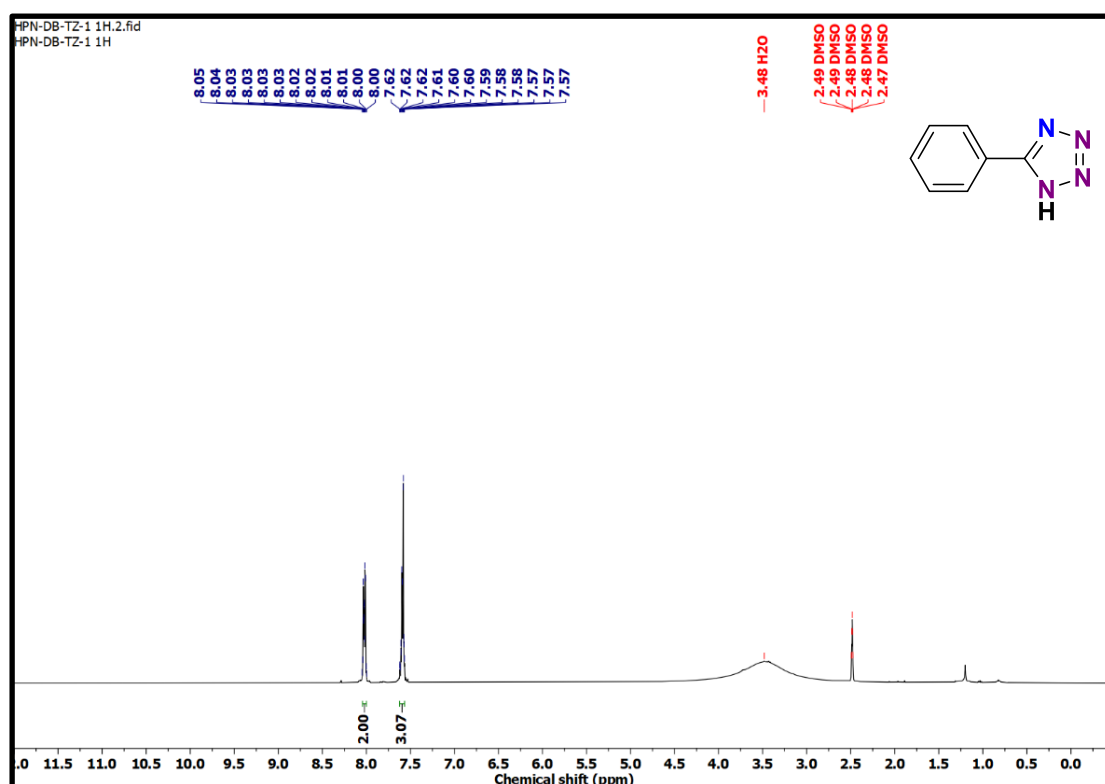


Figure S20. ¹H NMR (400 MHz, DMSO-*d*₆) spectrum of **4a**.

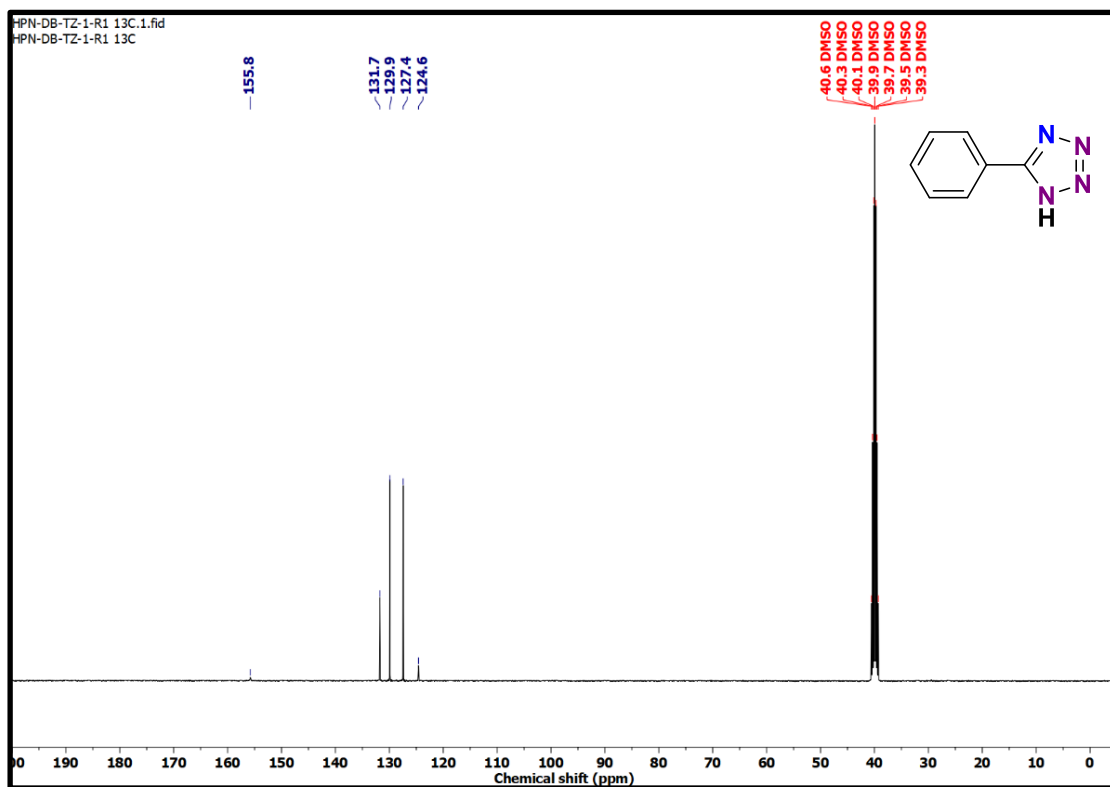


Figure S21. $^{13}\text{C}\{^1\text{H}\}$ NMR (100 MHz, $\text{DMSO-}d_6$) spectrum of **4a**.

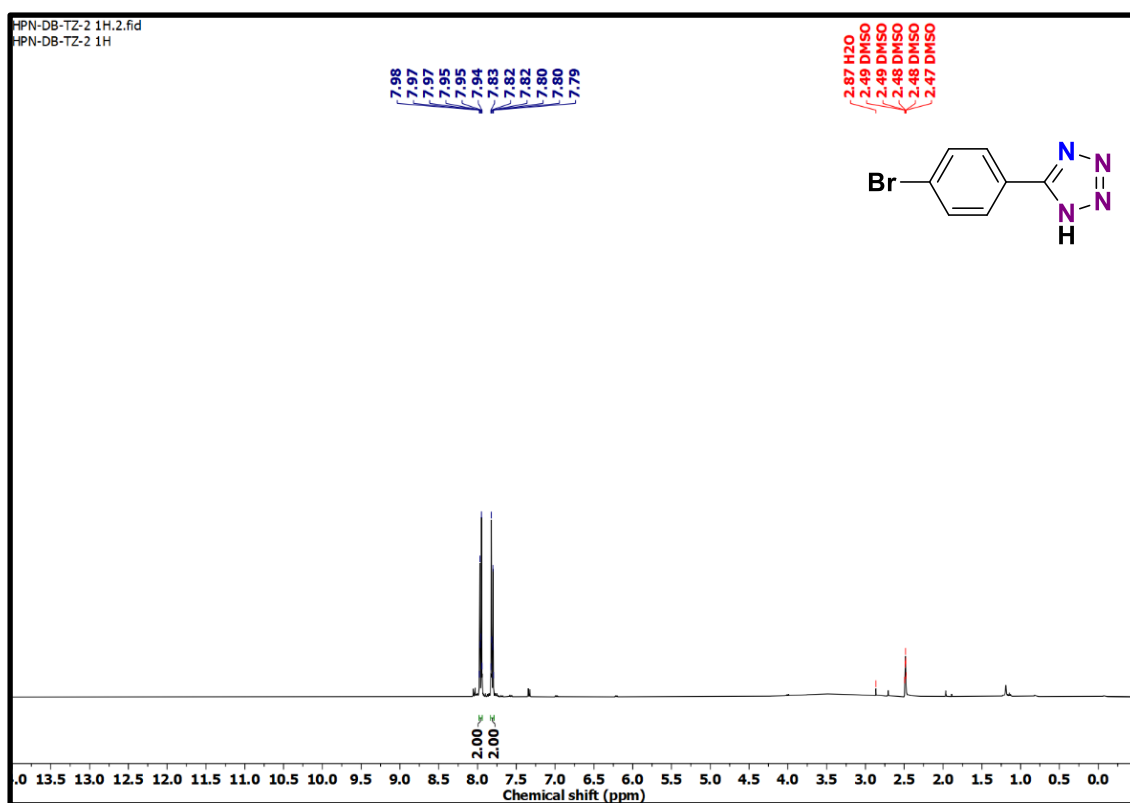


Figure S22. ^1H NMR (400 MHz, $\text{DMSO-}d_6$) spectrum of **4b**.

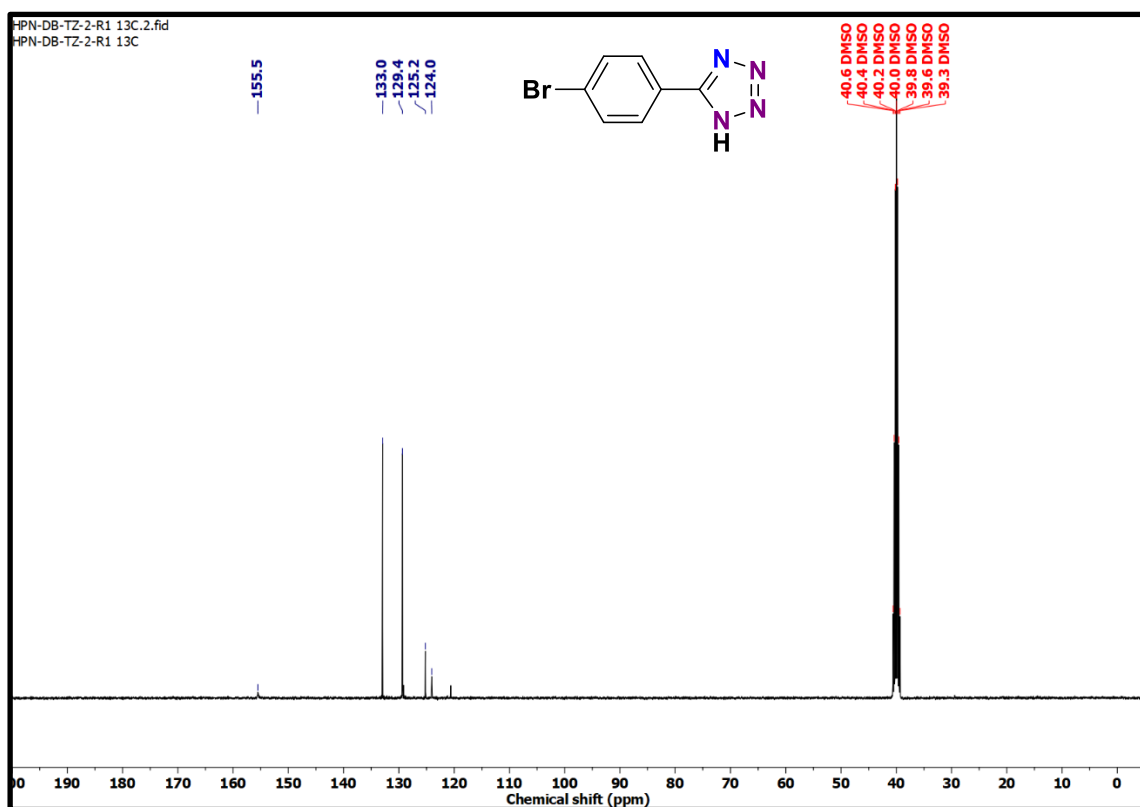


Figure S23. $^{13}\text{C}\{^1\text{H}\}$ NMR (100 MHz, $\text{DMSO-}d_6$) spectrum of **4b**.

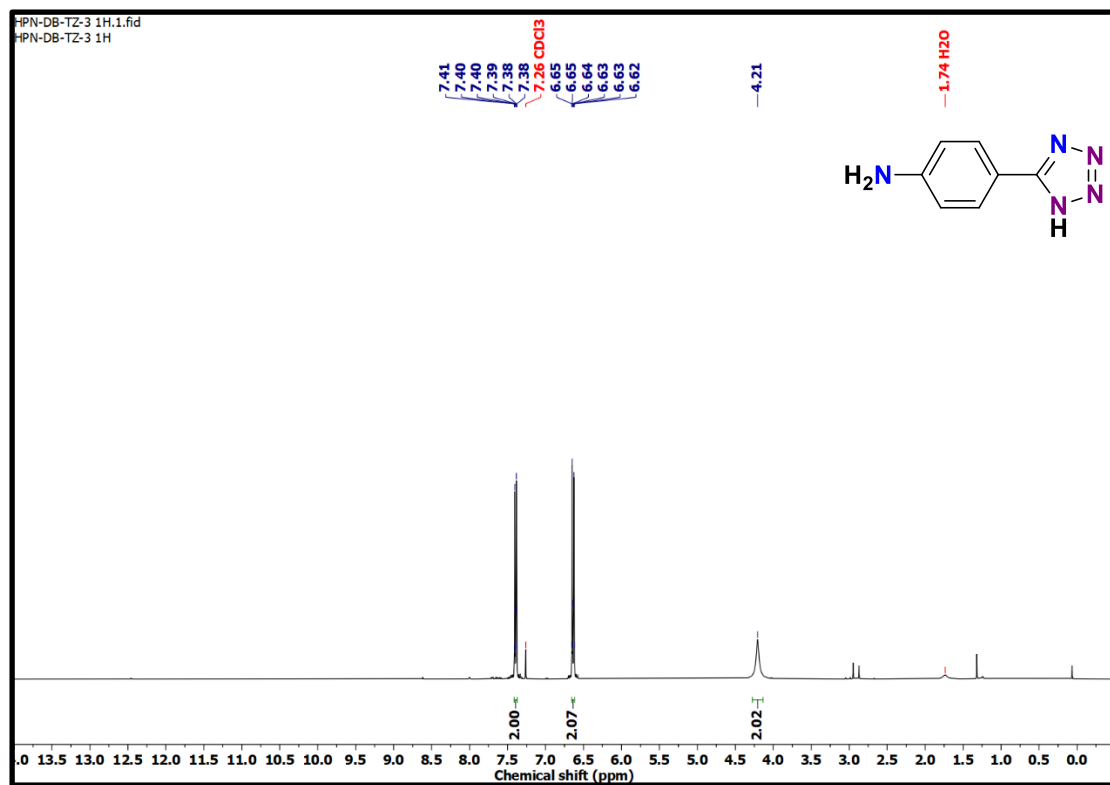


Figure S24. ^1H NMR (400 MHz, CDCl_3) spectrum of **4c**.

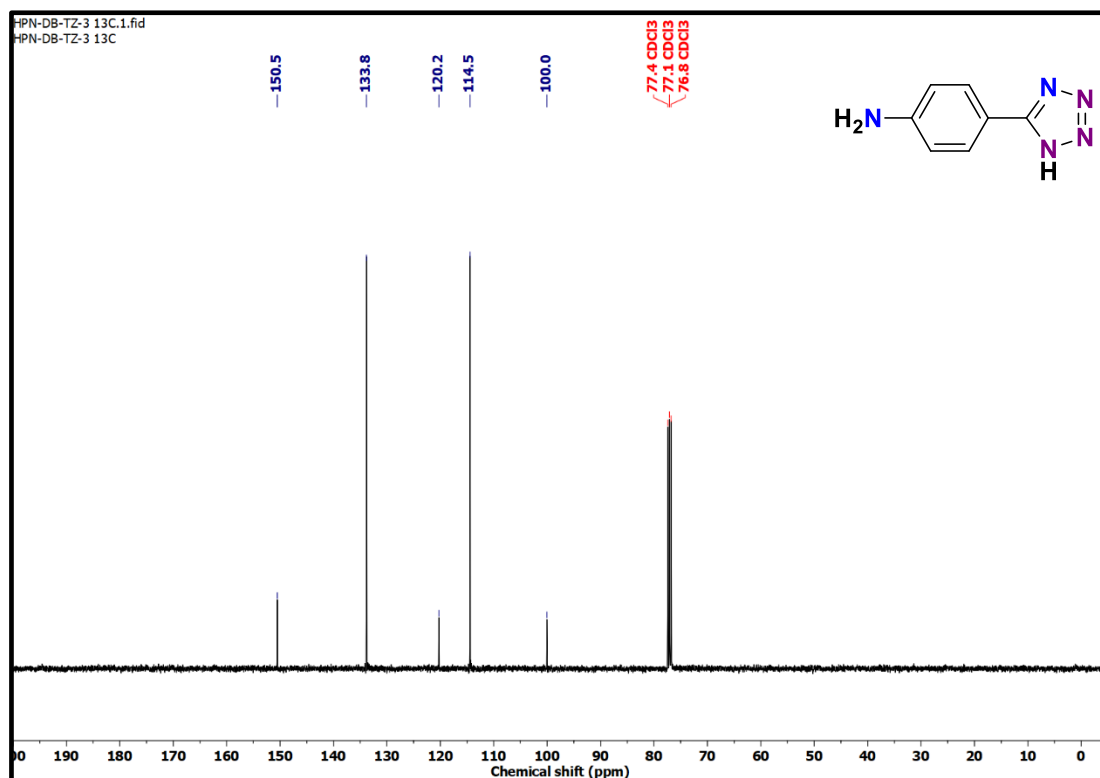


Figure S25. $^{13}\text{C}\{^1\text{H}\}$ NMR (100 MHz, CDCl_3) spectrum of **4c**.

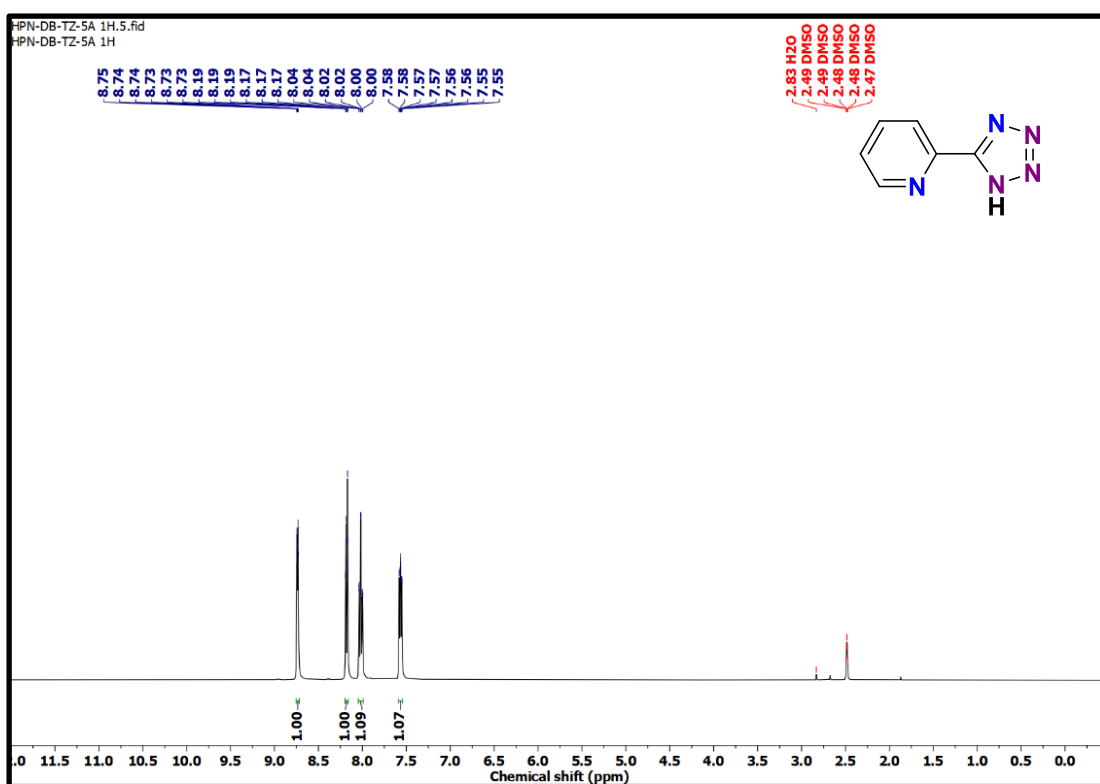


Figure S26. ^1H NMR (400 MHz, $\text{DMSO}-d_6$) spectrum of **4d**.

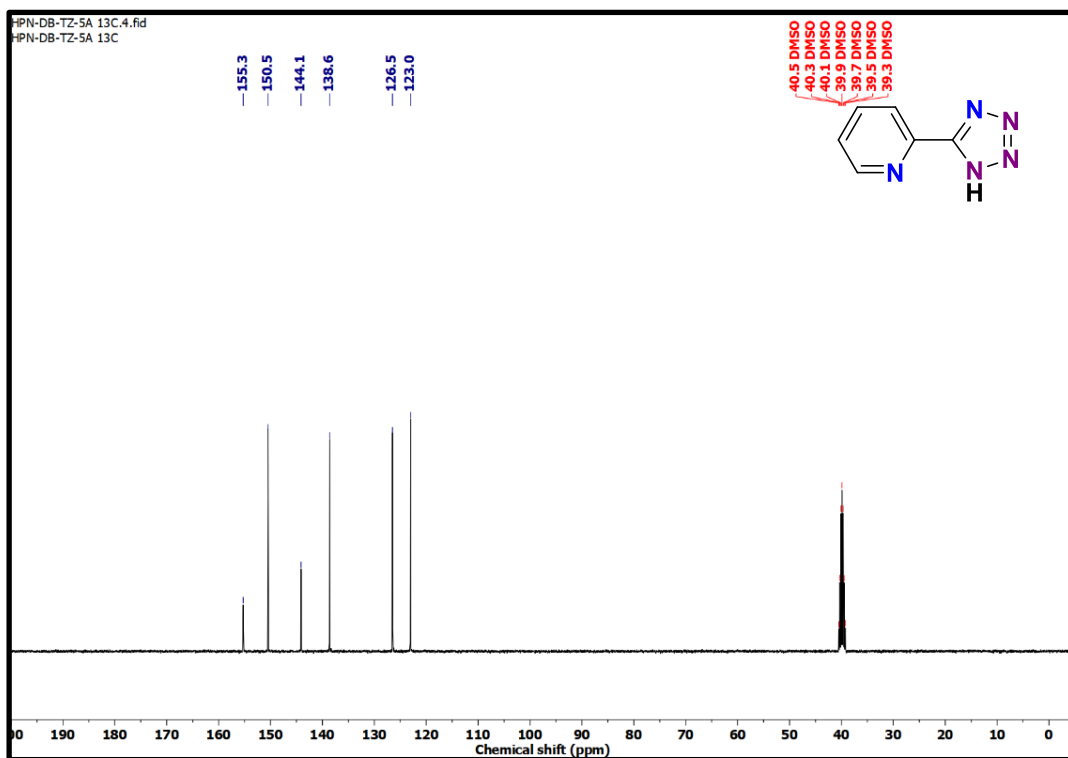


Figure S27. $^{13}\text{C}\{^1\text{H}\}$ NMR (100 MHz, $\text{DMSO-}d_6$) spectrum of 4d.

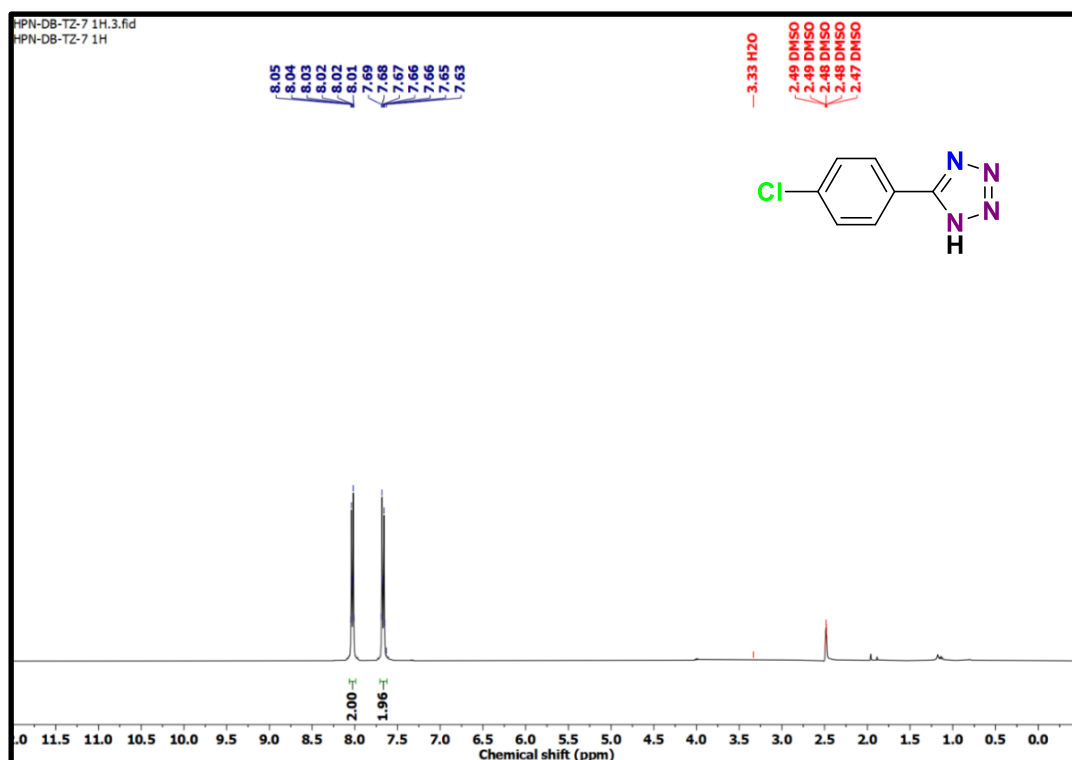


Figure S28. ^1H NMR (400 MHz, $\text{DMSO-}d_6$) spectrum of 4e.

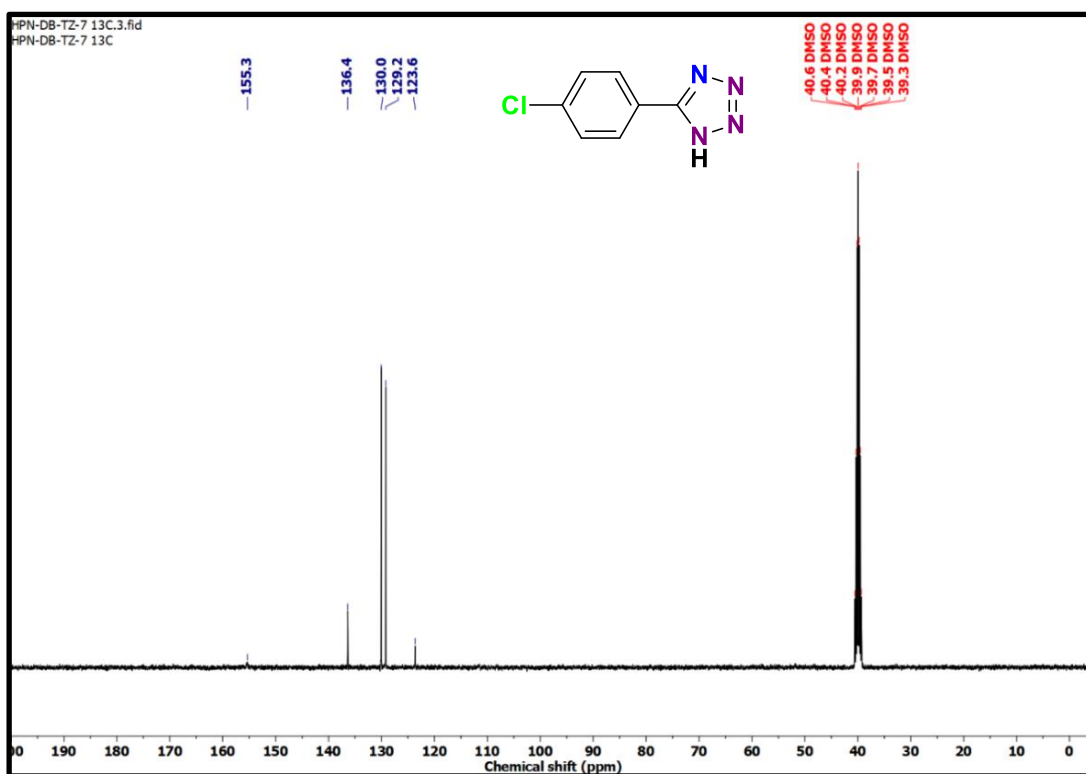


Figure S29. $^{13}\text{C}\{^1\text{H}\}$ NMR (100 MHz, $\text{DMSO-}d_6$) spectrum of 4e.

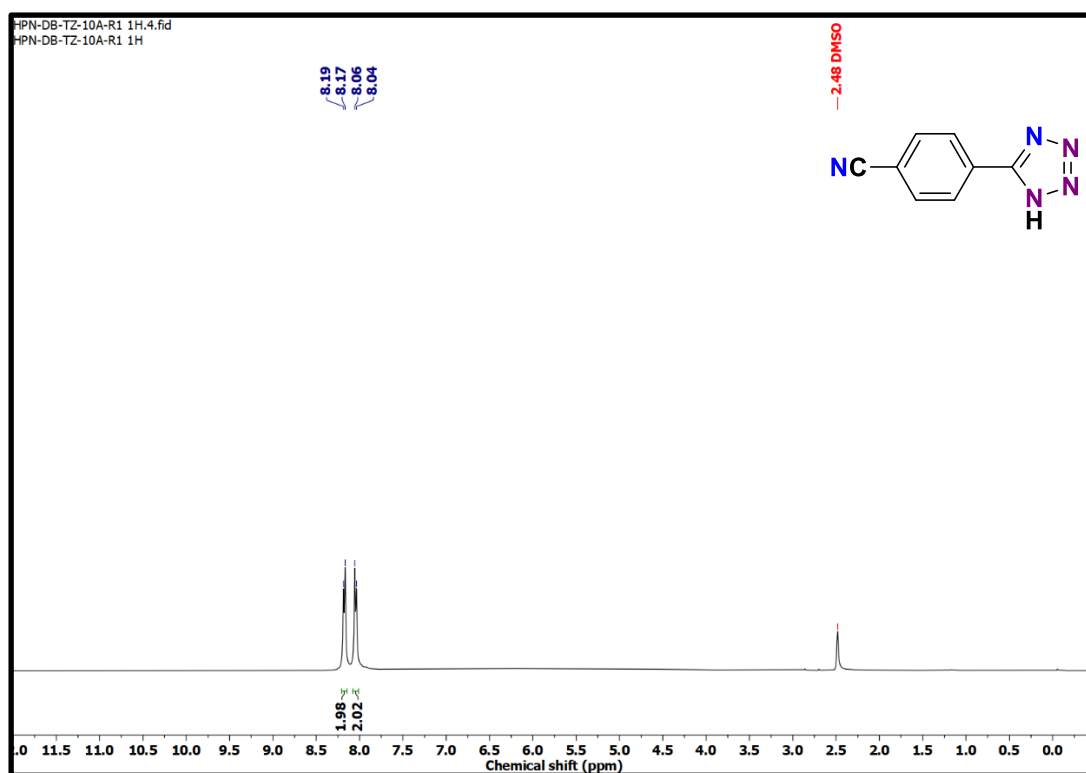


Figure S30. ^1H NMR (400 MHz, $\text{DMSO-}d_6$) spectrum of 4f.

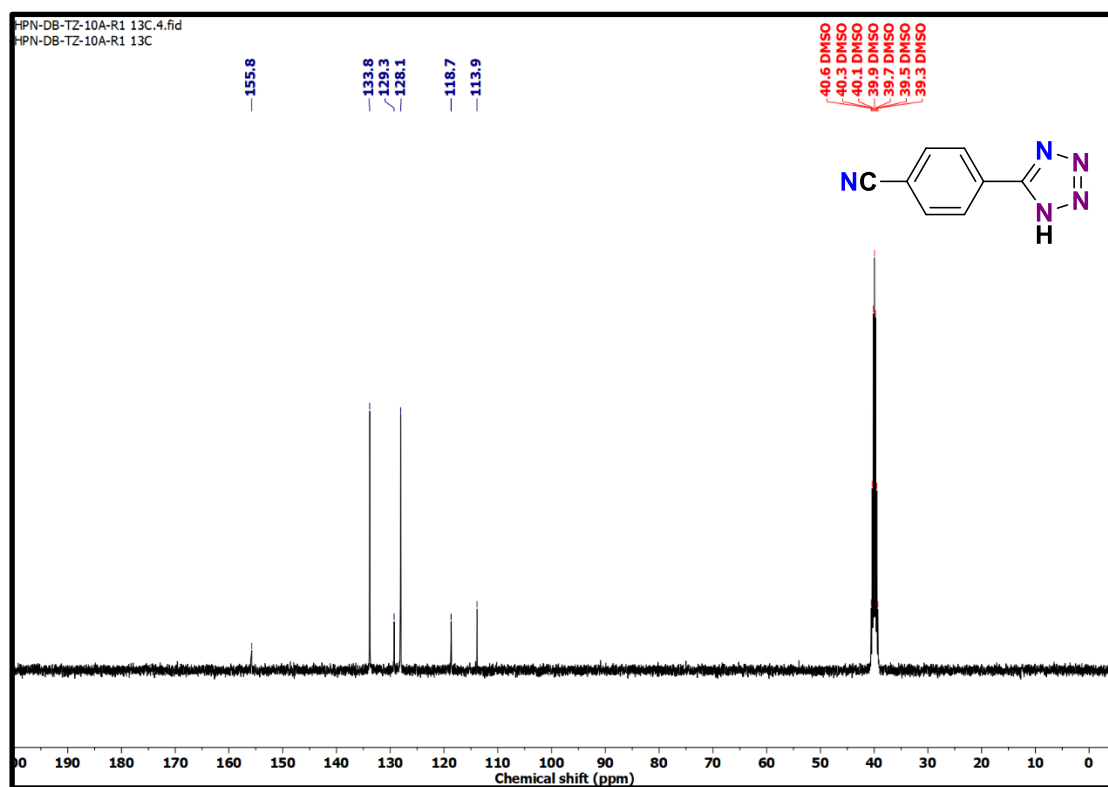


Figure S31. ^{13}C $\{^1\text{H}\}$ NMR (100 MHz, $\text{DMSO-}d_6$) spectrum of 4f.

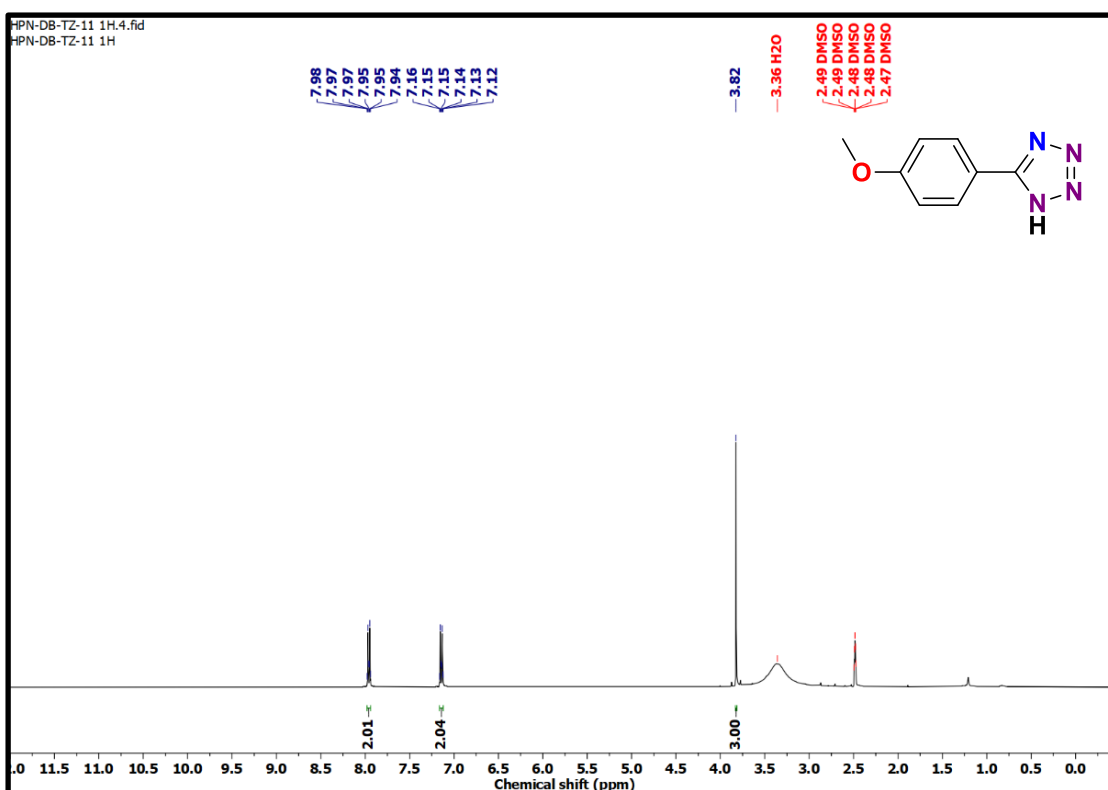


Figure S32. ^1H NMR (400 MHz, $\text{DMSO-}d_6$) spectrum of 4g.

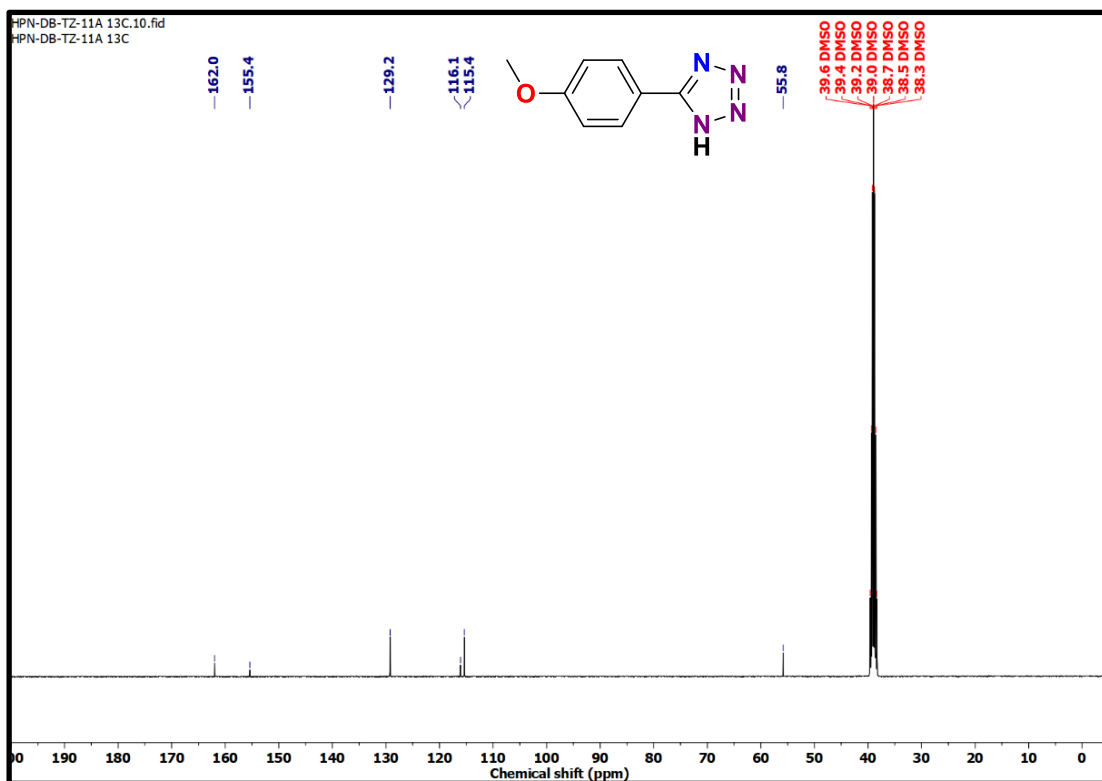


Figure S33. $^{13}\text{C}\{^1\text{H}\}$ NMR (100 MHz, $\text{DMSO-}d_6$) spectrum of **4g**.

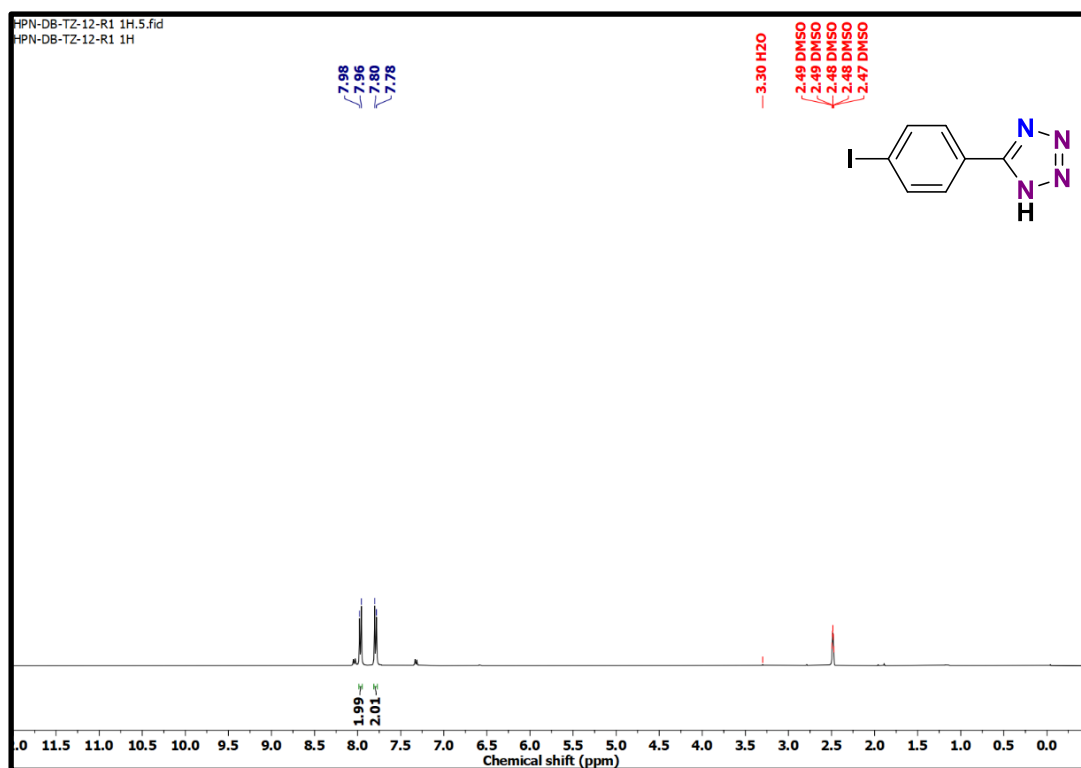


Figure S34. ^1H NMR (400 MHz, $\text{DMSO-}d_6$) spectrum of **4h**.

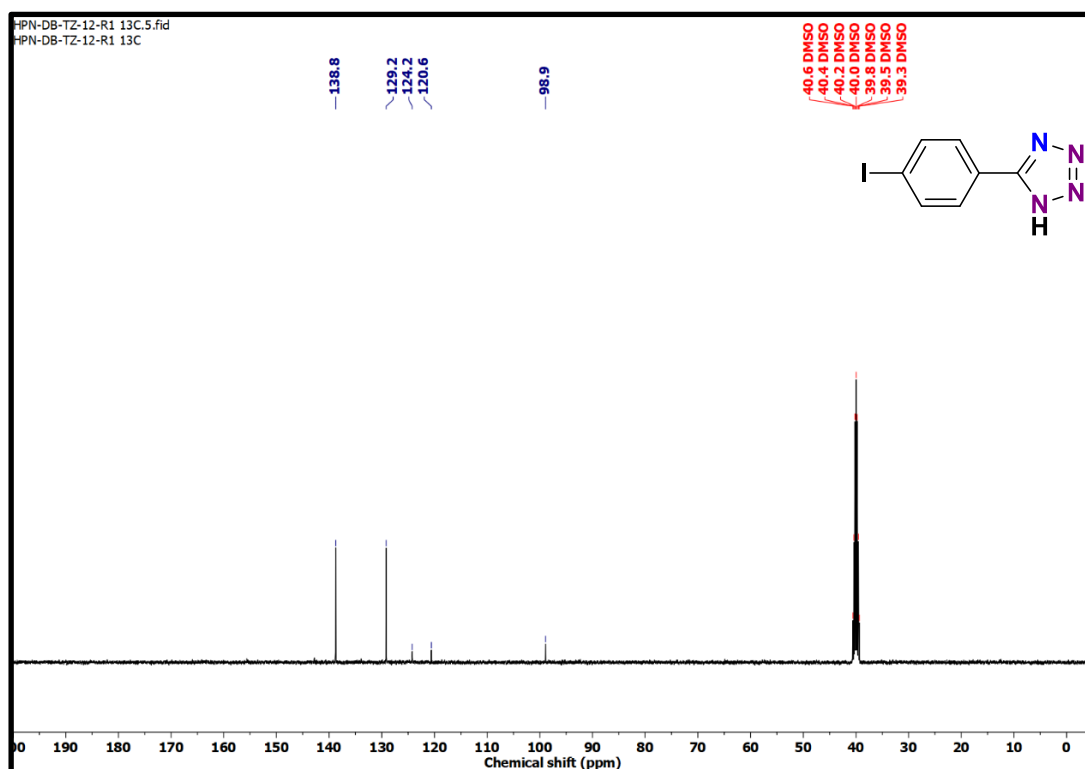


Figure S35. $^{13}\text{C}\{^1\text{H}\}$ NMR (100 MHz, $\text{DMSO-}d_6$) spectrum of 4h.

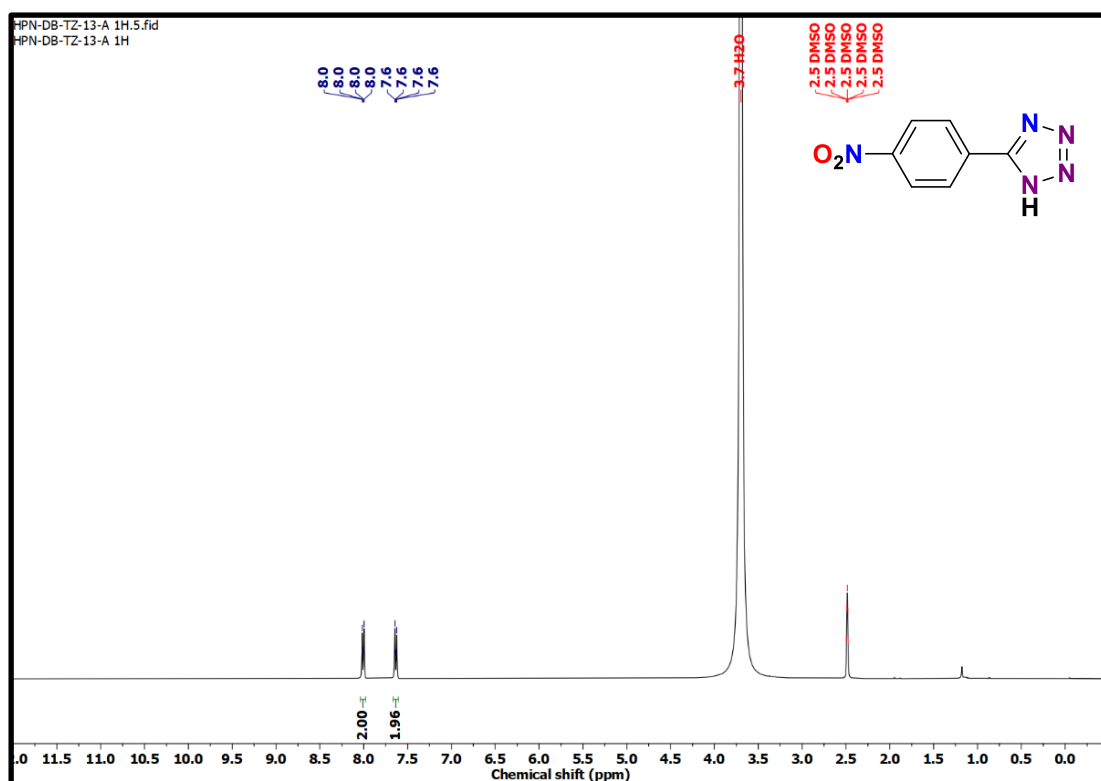


Figure S36. ^1H NMR (400 MHz, $\text{DMSO-}d_6$) spectrum of 4i.

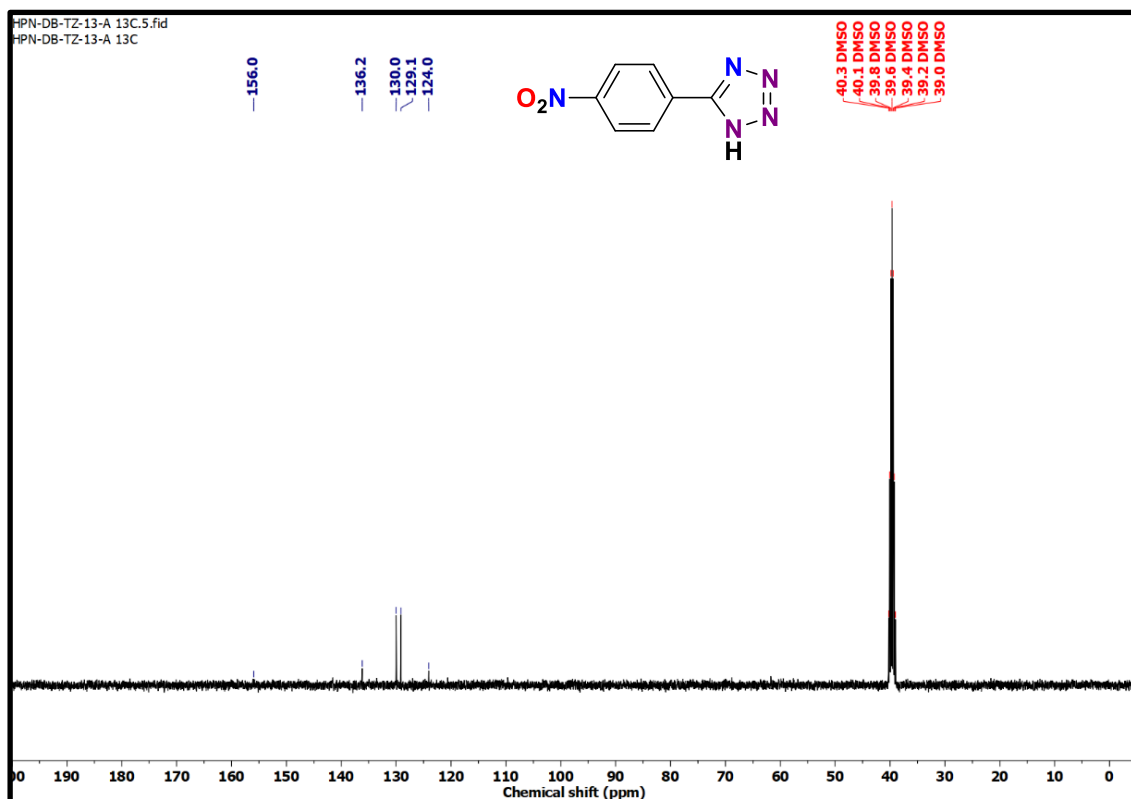


Figure S37. $^{13}\text{C}\{^1\text{H}\}$ NMR (100 MHz, $\text{DMSO}-d_6$) spectrum of **4i6**.

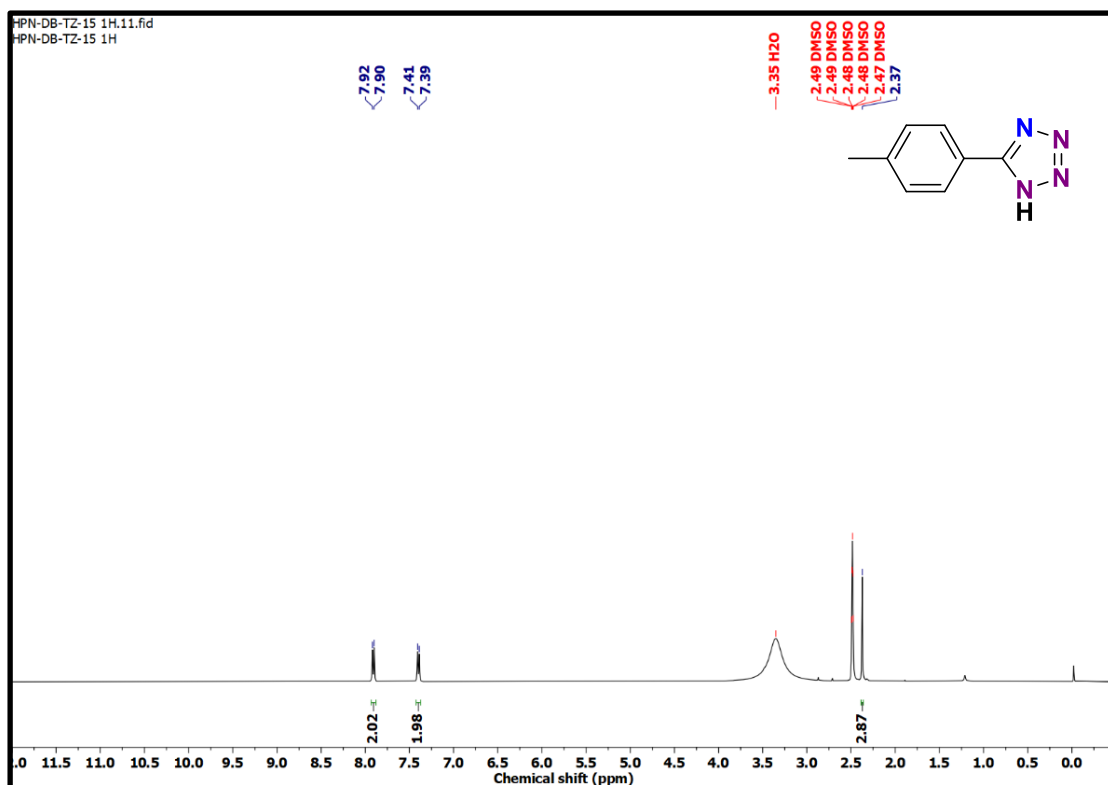


Figure S38. ^1H NMR (400 MHz, $\text{DMSO}-d_6$) spectrum of **4j**.

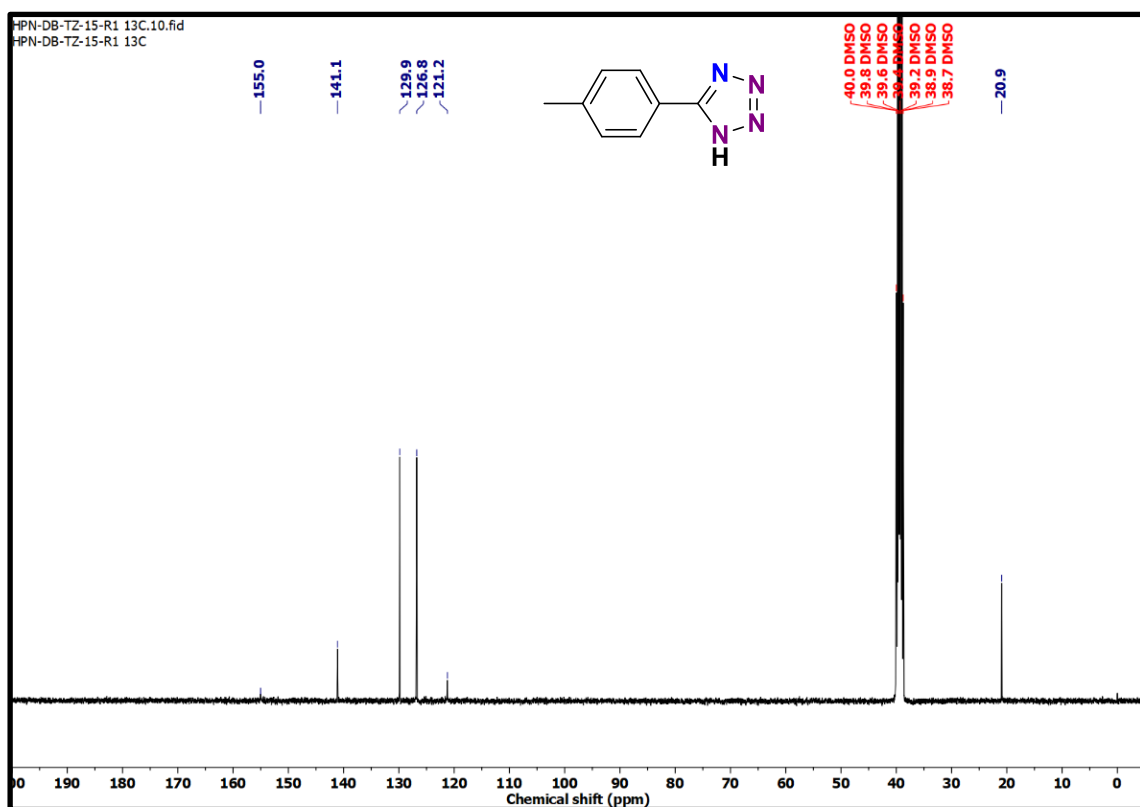


Figure S39. $^{13}\text{C}\{^1\text{H}\}$ NMR (100 MHz, $\text{DMSO-}d_6$) spectrum of **4j**.

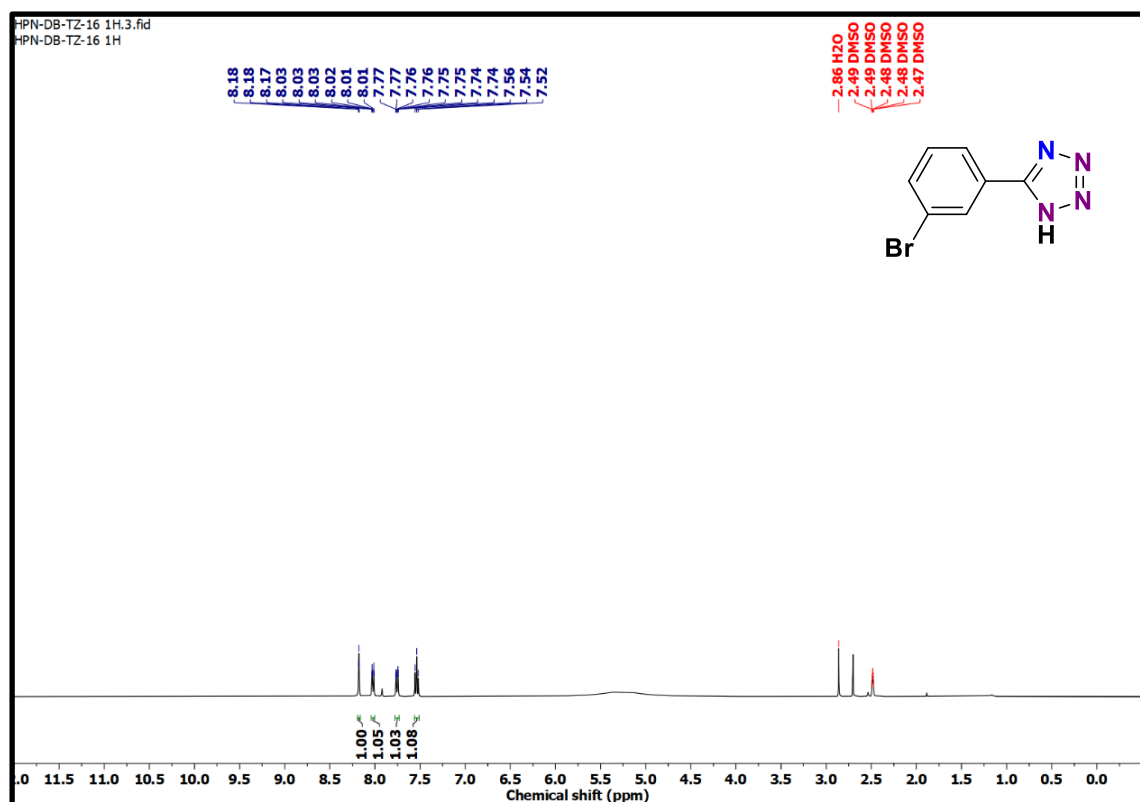


Figure S40. ^1H NMR (400 MHz, $\text{DMSO-}d_6$) spectrum of **4k**.

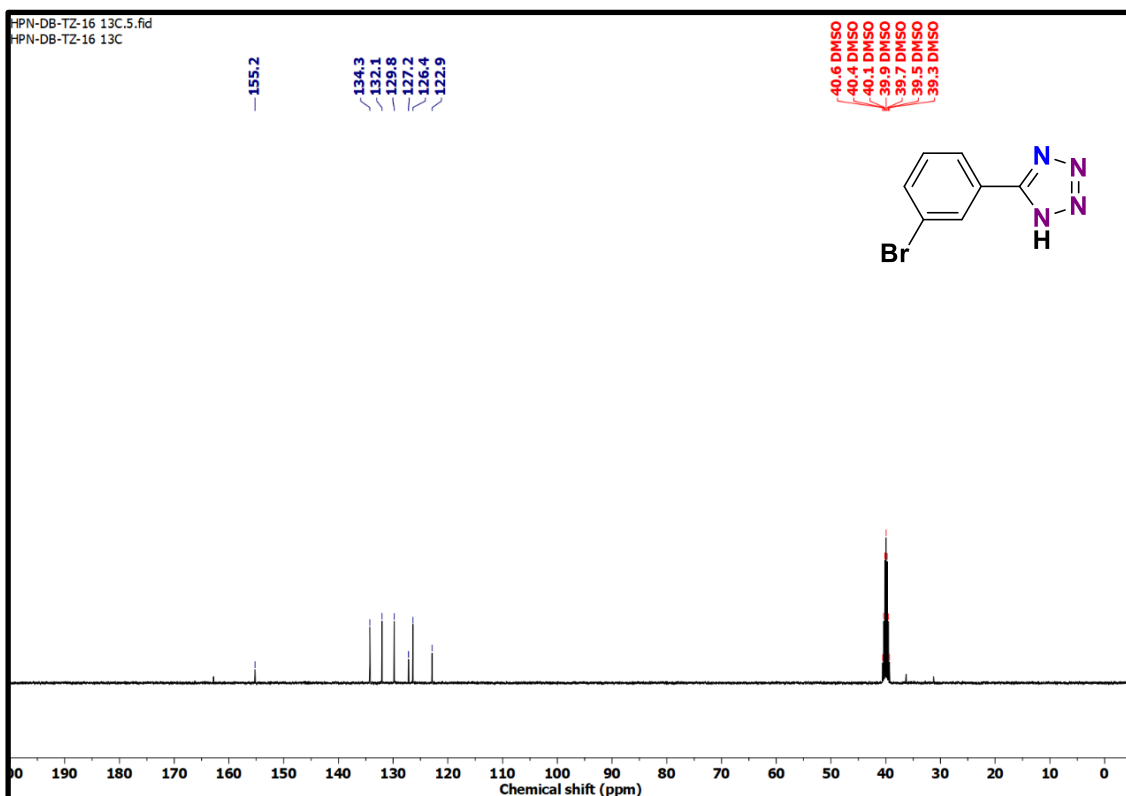


Figure S41. $^{13}\text{C}\{^1\text{H}\}$ NMR (100 MHz, $\text{DMSO-}d_6$) spectrum of **4k**.

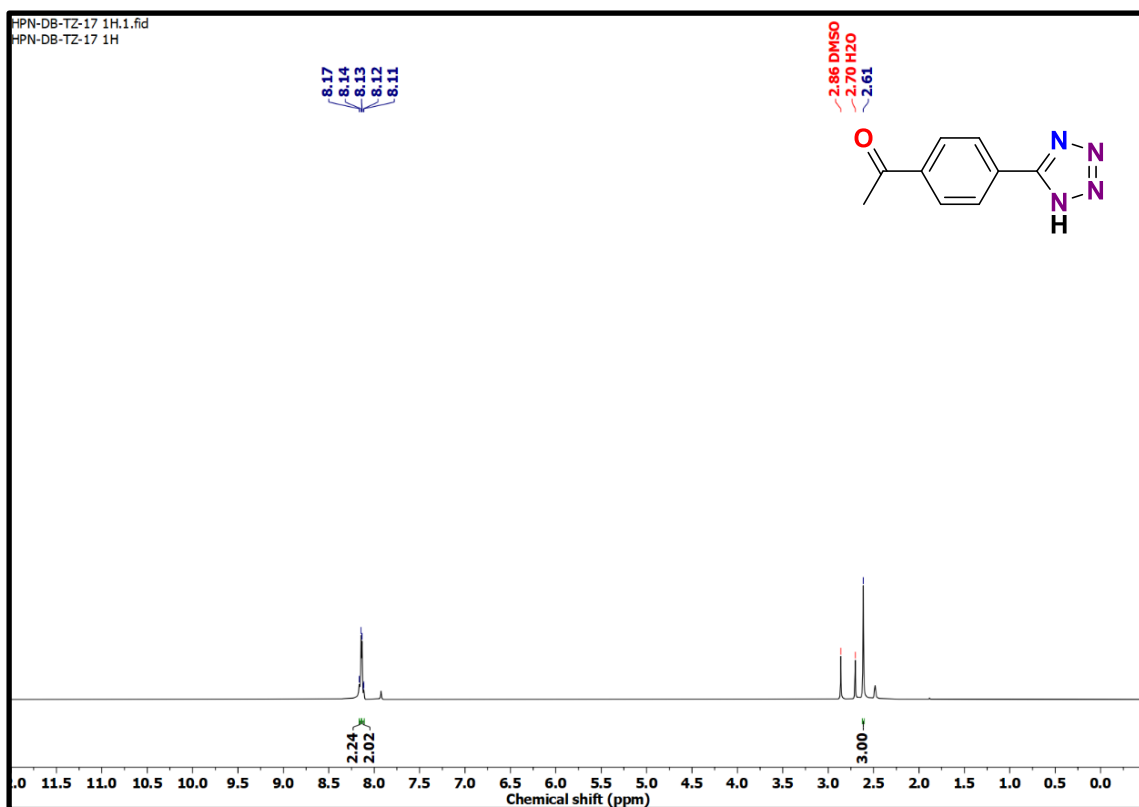


Figure S42. ^1H NMR (400 MHz, $\text{DMSO-}d_6$) spectrum of **4l**.

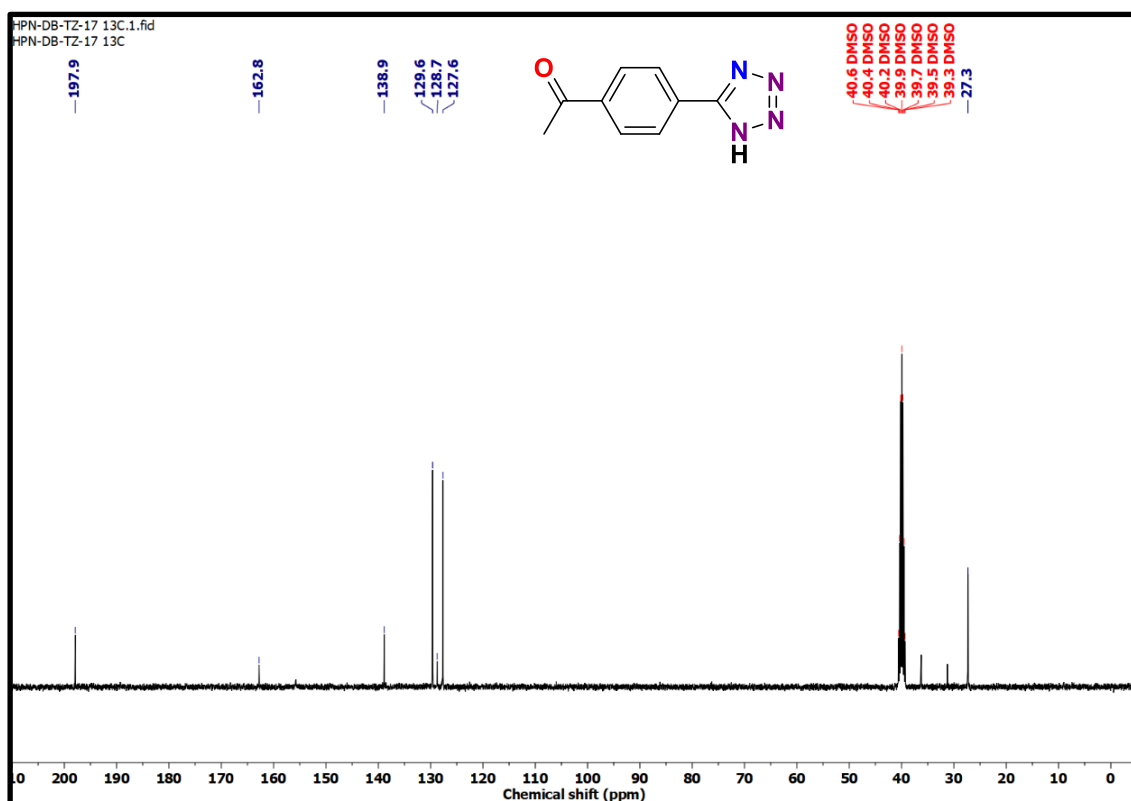


Figure S43. $^{13}\text{C}\{^1\text{H}\}$ NMR (100 MHz, $\text{DMSO-}d_6$) spectrum of **4l**.

DFT Methods

Gaussian 09 package⁶ was used to perform all the density functional theory (DFT) calculations using B3LYP-D3BJ functional⁷⁻¹⁰, where D3BJ accounted for dispersion correction using a combination of D3 and Becke–Johnson damping scheme. Pople style basis set 6-311+G(d,p)¹¹⁻¹⁴ was used for all gas phase geometric optimizations and frequency calculations under harmonic approximation at 373.15 K. Each intermediate and transition state was classified by the absence and presence of a single imaginary frequency in the optimized geometry respectively. A pruned (99, 590) grid (Gaussian’s ultrafine grid option) was used for computing numerical integrals, and convergence cutoffs on forces and step size during optimization were set using the opt=tight option enabled. Corroboration of the transition state between the reactant and product state was verified using intrinsic reaction calculation.¹⁵ The thermochemistry of each stationary state was worked out using the results of the frequency calculations. The obtained Free energy was refined further by considering the errors associated with the rigid rotor harmonic oscillator (RRHO) approximation considered during the frequency calculations using Truhlar’s quasi-harmonic approximation¹⁶ for vibrational entropy. During the correction, performed using GoodVibes code,¹⁷ all the vibrational frequencies $< 100\text{ cm}^{-1}$ were scaled to 100 cm^{-1} .

Gibbs free energy of gas phase H^+ ($G(\text{H}^+)$) was computed using the method described in Moser *et al.*¹⁸ using equations 1, 2,¹⁹ and 3.

$$\text{Enthalpy } H(H^+) = \frac{5}{2}RT \text{ (Equation 1)}$$

$$\text{Entropy } S(H^+) = R \ln \left(\frac{e^{\frac{5}{2}} k_b T}{p \Lambda^3} \right) \text{ (Equation 2)}$$

$$G(H^+) = H(H^+) - TS(H^+) \text{ (Equation 3)}$$

where k_b is the Boltzmann constant, Λ is the thermal de Broglie wavelength, h is the Planck's constant, and m is the proton's mass. The values of $H(H^+)$ and $S(H^+)$ were found to be 1.85 kcal/mol and 27.13 cal/(mol. K) under standard state conditions, resulting in $G(H^+) = -8.27$ kcal/mol. Gauss View 5.0.9 program²⁰ was used for input file preparation, visualization and analysis purposes.

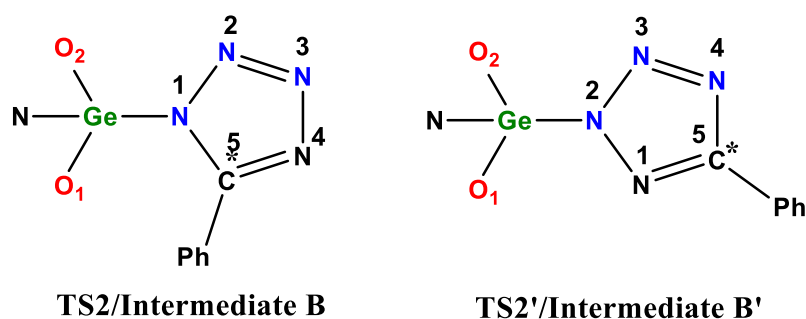


Figure S44. 1,5-disubstituted intermediate (**B**) and 2,5-disubstituted Intermediate (**B'**) with numbering scheme in Path I and Path II.

Table S4. Bond Lengths present in various stationary states. All values are reported in Å.

	Compound 1	TS1	A	PhCN	N ₃ ⁻	TS2	TS2'	B	B'	Product
Ge-N	2.02	2.13	2.13	-	-	2.13	2.13	2.11	2.12	-
Ge-O1	2.0	1.96	2.09	-	-	2.04	2.0	2.03	2.01	-
Ge-O2	1.97	1.91	2.03	-	-	2.09	2.04	2.08	2.06	-
Ge-N1	-	2.93	2.02	-	-	2.05	-	2.09	-	-
Ge-N2	-	2.93	2.02	-	-	-	2.10	-	2.09	-
*C-N4	-	-	-	1.16	-	1.2	-	1.33	-	1.35
*C-N1	-	-	-	1.16	-	-	1.20	-	1.33	1.35

N1- N2	-	1.18	1.2	-	1.18	1.25	-	1.35	-	1.36
N2- N3	-	1.18	1.2	-	1.18	-	1.2	-	1.33	1.36
N2- N3	-	1.18	1.15	-	1.18	1.17	-	1.3	-	1.29
N3- N4	-	1.18	1.15	-	1.18	-	1.2	-	1.32	1.29
N3- N4	-	-	-	-	-	2.07	-	1.35	-	1.35
N1- *C	-	-	-	-	-	1.89	-	1.36	-	1.32
N4- *C	-	-	-	-	-	-	1.82	-	1.36	1.32
N1- N2	-	-	-	-	-	-	2.18	-	1.33	1.35

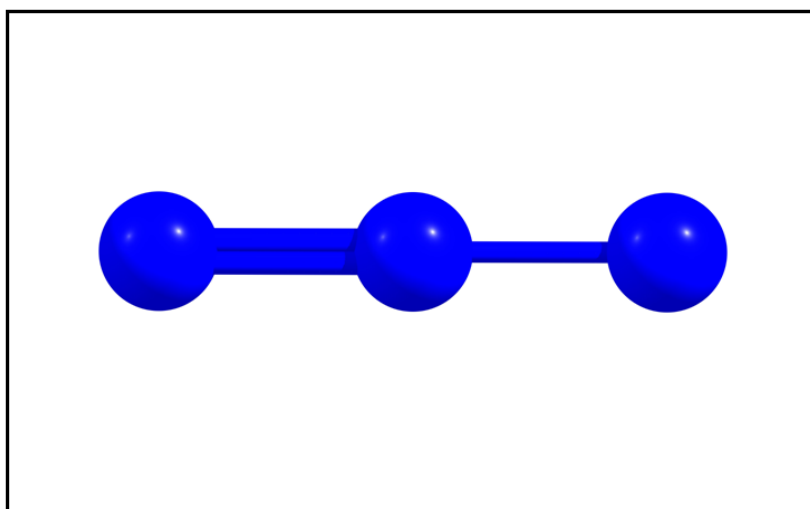


Figure S45. DFT-optimized geometry of azide ion.

Table S5. Cartesian coordinates of DFT-optimized geometry of azide ion.

N_3^-

N	0.00000000	0.00000000	0.00000000
N	0.00000000	0.00000000	1.18320600
N	0.00000000	0.00000000	-1.18320600

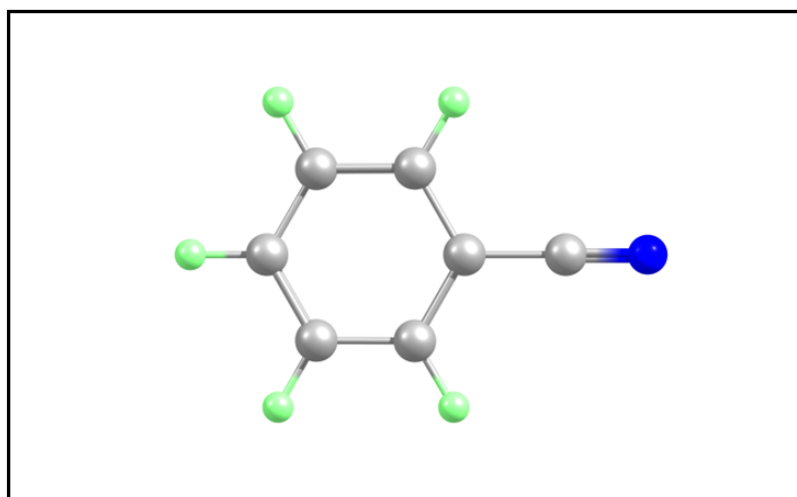


Figure S46. DFT-optimized geometry of benzonitrile.

Table S6. Cartesian coordinates of DFT-optimized geometry of benzonitrile.

C₇H₅N

C	0.00000000	-0.60943600	0.00000000
C	1.21485200	0.08972700	0.00000000
C	1.20845100	1.47948100	0.00000000
C	0.00000000	2.17488500	0.00000000
C	-1.20845100	1.47948100	0.00000000
C	-1.21485200	0.08972700	0.00000000
H	2.14746800	-0.45992800	0.00000000
H	2.14706600	2.02021000	0.00000000
H	0.00000000	3.25841100	0.00000000
H	-2.14706600	2.02021000	0.00000000
H	-2.14746800	-0.45992800	0.00000000
C	0.00000000	-2.03960500	0.00000000
N	0.00000000	-3.19493300	0.00000000

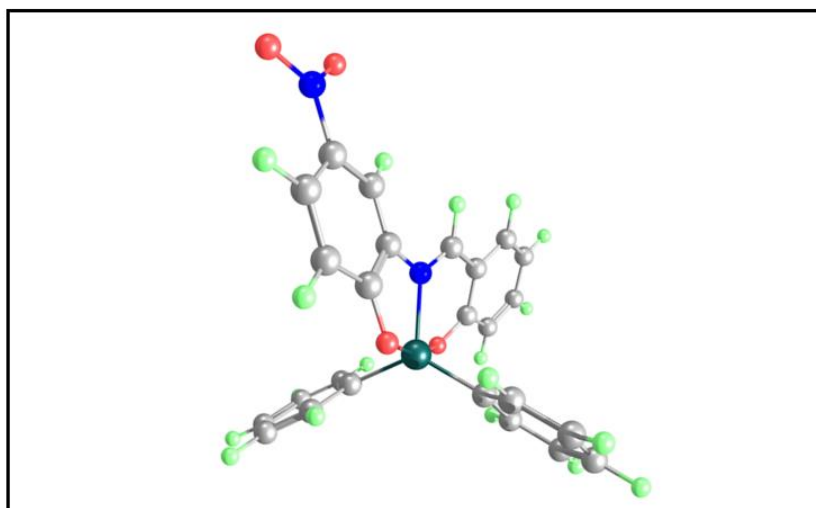


Figure S47. DFT-optimized geometry of compound 1.

Table S7. Cartesian coordinates of DFT-optimized geometry of compound 1 [Ge(IV) compound].

C₂₅H₁₈N₂O₄Ge

C	-1.89973600	-0.71850300	1.02426100
C	-1.88727500	0.45461500	0.22167700
C	-3.05656800	1.11050700	-0.11779700
C	-4.25852000	0.61326700	0.38111500
C	-4.30414700	-0.52922400	1.18632300
C	-3.13418200	-1.19607600	1.50153300
N	-5.49793400	1.29757600	0.03148200
O	-5.42126800	2.30107800	-0.67665900
O	-6.55180000	0.83947000	0.46479300
O	-0.75262100	-1.28557900	1.28632600
N	-0.58587800	0.82060300	-0.18173900
H	-3.07478900	1.97586800	-0.76537800
H	-5.26262700	-0.87921900	1.54311200
H	-3.14463900	-2.08610100	2.11702200
Ge	0.75051200	-0.66106700	0.11631900
C	-0.27983200	2.04953400	-0.51099200
H	0.35109000	4.57083900	-0.93209400
C	1.16517200	3.89676800	-1.17725600

C	2.35142800	4.38822400	-1.66926900
H	2.49103000	5.45159300	-1.81358400
C	3.38365800	3.48516300	-1.99211200
H	4.31940000	3.86646300	-2.38563200
C	3.22966500	2.12401500	-1.82024400
H	4.02037600	1.42907400	-2.07385800
C	2.02797600	1.59550500	-1.30211400
C	0.97725900	2.50634300	-0.97888000
O	1.89069000	0.30356500	-1.16893400
H	-1.06720000	2.79581300	-0.41261900
H	1.56036600	-1.28430500	-2.74431400
C	1.11333100	-2.19081300	-2.36074700
C	0.63090900	-2.22141500	-1.04716700
C	0.06665100	-3.40584500	-0.55544000
H	-0.31902700	-3.43677900	0.45463400
C	-0.01077500	-4.53767900	-1.36352400
H	-0.44635900	-5.44956300	-0.97119800
C	0.46420900	-4.49680200	-2.67260800
H	0.39789000	-5.37644900	-3.30276200
C	1.02386000	-3.32185000	-3.16955500
H	1.39398000	-3.28469600	-4.18788800
C	1.96337800	-0.38017100	1.61769700
C	3.32738300	-0.16814500	1.38044200
H	3.70095100	-0.15749000	0.36503600
C	4.20597500	0.03137700	2.44240400
H	5.26042700	0.18976000	2.24676700
C	3.73038500	0.03076100	3.75220300
H	4.41364800	0.19123900	4.57840700
C	2.37517800	-0.17938500	3.99717300
H	2.00140500	-0.18387700	5.01480500
C	1.49577400	-0.39031400	2.93695800
H	0.44743700	-0.57269500	3.13045200

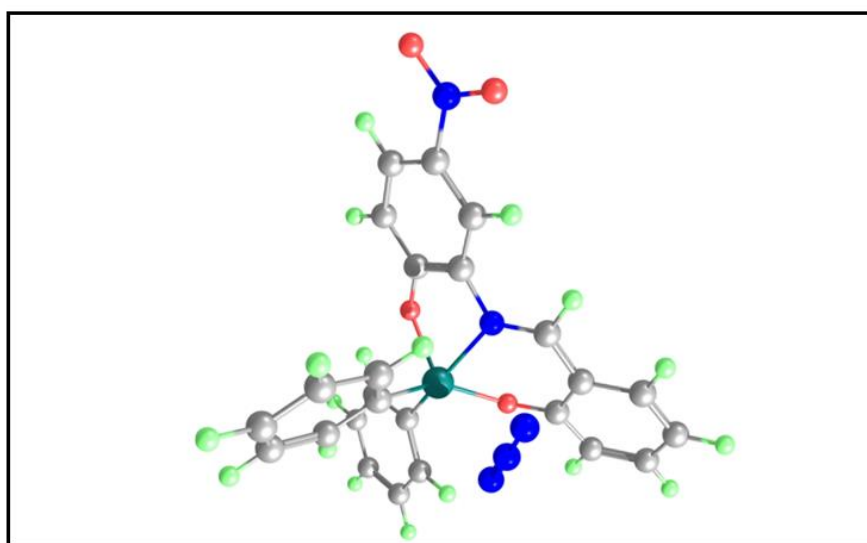


Figure S48. DFT-optimized geometry of compound **1** and azide (Transition state 1).

Table S8. Cartesian coordinates of DFT-optimized geometry of compound **1** and azide (Transition state 1).

$C_{25}H_{18}N_2O_4Ge + N_3^-$

C	-1.57405500	-1.12937800	-1.30918600
C	-1.93717000	0.10557400	-0.68966300
C	-3.26365200	0.42797200	-0.47308400
C	-4.24826400	-0.47276400	-0.89040900
C	-3.92010400	-1.68146800	-1.51258200
C	-2.59186600	-2.00625300	-1.72277000
N	-5.64374100	-0.14172900	-0.67533500
O	-5.91413900	0.93777500	-0.14418100
O	-6.50191300	-0.95240500	-1.03673500
O	-0.30151900	-1.39392800	-1.47745500
N	-0.80987300	0.88027500	-0.40806200
H	-3.55868900	1.34653700	0.01397100
H	-4.71542500	-2.34754900	-1.81530800
H	-2.31120600	-2.93868900	-2.19544400
Ge	0.89819400	-0.38205200	-0.29770600

C	-0.82844500	2.16499900	-0.18609400
H	-0.68582100	4.72925400	0.41388400
C	0.25497100	4.34776500	0.03268300
C	1.33749100	5.18378900	-0.12931200
H	1.26218100	6.23676100	0.11317200
C	2.54742100	4.64766900	-0.60977200
H	3.40636700	5.29765300	-0.74159400
C	2.66482100	3.30448800	-0.90087100
H	3.59542700	2.87699600	-1.25224600
C	1.57749600	2.42617400	-0.70819200
C	0.34272400	2.97189400	-0.26416800
O	1.74508600	1.15668400	-1.03626000
H	-1.78149600	2.67353000	-0.04817700
H	3.82077400	-0.06836900	0.21541300
C	3.75847800	-0.96852300	-0.38572600
C	2.50929400	-1.39909200	-0.85029800
C	2.44453100	-2.56443300	-1.61883300
H	1.48349300	-2.90997900	-1.97834800
C	3.60298100	-3.28138100	-1.92493500
H	3.53743700	-4.18127100	-2.52832800
C	4.83999700	-2.84678200	-1.45412600
H	5.74009500	-3.40631900	-1.68696600
C	4.91460800	-1.68823000	-0.68017100
H	5.87415900	-1.34558000	-0.30659800
C	0.36546800	-1.21274600	1.41726500
C	-0.77055900	-0.85655400	2.15332500
H	-1.37113900	-0.00849300	1.86820000
C	-1.11816600	-1.55784800	3.30659200
H	-1.99246700	-1.25107300	3.87007300
C	-0.34393100	-2.62985800	3.74117700

H	-0.61727600	-3.17336900	4.63955300
C	0.79083100	-2.99297000	3.01727800
H	1.40813500	-3.82167100	3.34881400
C	1.14010700	-2.29039700	1.86692300
H	2.02754200	-2.58306700	1.32022400
N	1.70302100	1.40051200	1.88378900
N	0.68107700	1.80958900	2.31354100
N	-0.36683500	2.20927900	2.66935900

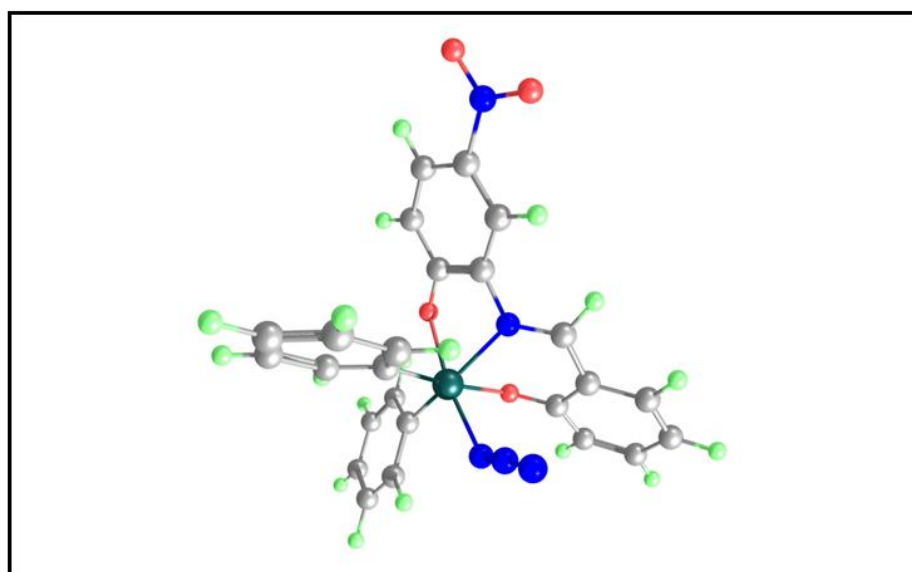


Figure S49. DFT-optimized geometry of compound **1** and azide (Intermediate A).

Table S9. Cartesian coordinates of DFT-optimized geometry of compound **1** and azide (Intermediate A).

C₂₅H₁₈N₅O₄Ge

C	-1.50726100	-0.60649100	-1.44777200
C	-1.80153800	0.51201600	-0.59292300
C	-3.09586100	0.90299300	-0.32939200
C	-4.14579900	0.19792500	-0.92858300
C	-3.89693400	-0.88794100	-1.78106200
C	-2.60067300	-1.28392400	-2.03803000
N	-5.50536000	0.59634100	-0.66034600

O	-5.70071100	1.55689900	0.09374400
O	-6.42369600	-0.03497000	-1.19676100
O	-0.27410900	-0.94168500	-1.63644000
N	-0.62324600	1.11941200	-0.14580600
H	-3.32072200	1.72965900	0.33037700
H	-4.73798100	-1.40711000	-2.21890300
H	-2.39118400	-2.12832200	-2.68241500
Ge	0.93008800	-0.32926400	-0.04349400
C	-0.46647000	2.38693900	0.07764300
H	0.14268200	4.80080300	1.01899000
C	0.97107600	4.33738800	0.49232000
C	2.14204900	5.03403800	0.28807400
H	2.25608200	6.04532000	0.65898500
C	3.18747300	4.41164100	-0.42349400
H	4.11111200	4.95500400	-0.59708400
C	3.06366900	3.12375300	-0.89920900
H	3.86834900	2.63760800	-1.43705500
C	1.89204600	2.35863900	-0.66201200
C	0.81678800	3.01055900	0.03772500
O	1.81666700	1.14551200	-1.11877700
H	-1.34567600	3.02801700	0.18057300
H	3.42770600	-1.35240500	1.29312100
C	3.44850000	-1.79826800	0.30567200
C	2.42256800	-1.50459500	-0.59790800
C	2.46933200	-2.07785800	-1.87269500
H	1.67739400	-1.86349100	-2.57876700
C	3.51650900	-2.92514700	-2.23524000
H	3.53775400	-3.36155500	-3.22904100
C	4.53266400	-3.21444800	-1.32555600
H	5.34637000	-3.87538500	-1.60636400

C	4.49545700	-2.64754100	-0.05268100
H	5.28284800	-2.86493000	0.66221100
C	-0.19111800	-1.51603700	1.13402500
C	-1.07432000	-1.04223200	2.11051600
H	-1.19884900	0.02201800	2.26302500
C	-1.81242500	-1.92029000	2.90381700
H	-2.49237700	-1.52694000	3.65226200
C	-1.68092700	-3.29657100	2.73254900
H	-2.25758500	-3.98138800	3.34551200
C	-0.80458300	-3.78555200	1.76492200
H	-0.69499900	-4.85603200	1.62172300
C	-0.07023900	-2.90127700	0.97586700
H	0.60484400	-3.29607100	0.22470900
N	1.84130500	0.54074200	1.54121600
N	1.26584600	1.08587900	2.44509900
N	0.76664200	1.63181200	3.32503400

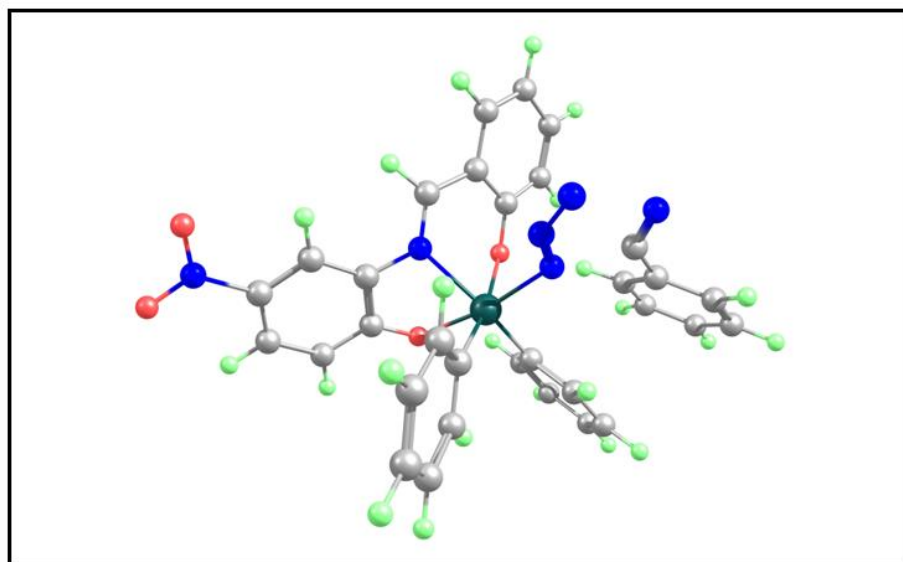


Figure S50. DFT-optimized geometry of Str A and benzonitrile (Transition state 2).

Table S10. Cartesian coordinates of DFT-optimized geometry of Str A and benzonitrile (Transition state 2).

C₂₅H₁₈N₅O₄Ge + C₇H₅N

C	-2.50148100	-0.69361700	-1.39948000
C	-2.72812600	0.45153600	-0.56092200
C	-3.99425000	0.83300700	-0.17681800
C	-5.08663400	0.09024800	-0.63867800
C	-4.90655800	-1.02170600	-1.47458000
C	-3.63661300	-1.40801400	-1.85062600
N	-6.41858100	0.47656200	-0.24268300
O	-6.55238300	1.46111500	0.49336700
O	-7.37478900	-0.18902900	-0.65670500
O	-1.28620900	-1.01752900	-1.69584400
N	-1.52031300	1.09576300	-0.26463500
H	-4.16476400	1.67955400	0.47395700
H	-5.77855700	-1.56894100	-1.80440800
H	-3.47879300	-2.27232800	-2.48314700
Ge	0.05019200	-0.34542400	-0.23625600
C	-1.36958800	2.37544700	-0.14737900
H	-0.72610400	4.85312300	0.57299600
C	0.05469600	4.37206200	-0.00761100
C	1.17707100	5.07818100	-0.38259600
H	1.30512500	6.11199800	-0.08686200
C	2.14888500	4.43480500	-1.16990600
H	3.03027900	4.98332700	-1.48566100
C	2.00774600	3.11435300	-1.54504600
H	2.75987700	2.62396800	-2.14979000
C	0.90099200	2.33910600	-1.11801600
C	-0.10934800	3.01515600	-0.35429000
O	0.82687700	1.08214000	-1.46489300
H	-2.24900600	3.01032200	-0.01190900

H	1.98980300	-2.20446600	1.11313200
C	2.15444500	-2.35791000	0.05241000
C	1.41329600	-1.62163900	-0.87521100
C	1.64437900	-1.82835200	-2.23659700
H	1.07061100	-1.26658300	-2.96330900
C	2.60620200	-2.74357300	-2.66187600
H	2.77930000	-2.89267000	-3.72309100
C	3.34786300	-3.46519600	-1.72701200
H	4.10393200	-4.16985400	-2.05726800
C	3.11870700	-3.27184900	-0.36658200
H	3.70021100	-3.81902800	0.36735400
C	-0.99358100	-1.44279200	1.09782100
C	-1.65626700	-0.91365400	2.20867100
H	-1.61426400	0.14970300	2.40776300
C	-2.38354500	-1.73015700	3.07382200
H	-2.89307100	-1.29304800	3.92616800
C	-2.46092000	-3.10161900	2.84090200
H	-3.02801200	-3.73901700	3.51104000
C	-1.81004600	-3.64548300	1.73514800
H	-1.86867900	-4.71142500	1.53917100
C	-1.08944200	-2.82055600	0.87259300
H	-0.60321600	-3.25523900	0.00696500
N	1.15439400	0.60131400	1.21464200
N	0.55573100	1.23253700	2.11596400
N	0.84110600	1.90053300	3.03904000
C	5.03952300	-0.18193600	1.58817600
C	6.04345000	-0.79744500	0.84815000
C	5.95010500	-0.85952900	-0.54191700
C	4.84257400	-0.31133700	-1.18304600
C	3.82750200	0.28943000	-0.44610800

C	3.92086300	0.36488200	0.94448500
H	5.10420200	-0.11883200	2.66725700
H	6.89862900	-1.22884000	1.35717800
H	6.72882600	-1.34607400	-1.11902300
H	4.74465700	-0.38192800	-2.25950600
H	2.94952400	0.66727200	-0.94447900
C	2.90918000	1.02379700	1.76890000
N	2.87893300	1.71545200	2.75160900

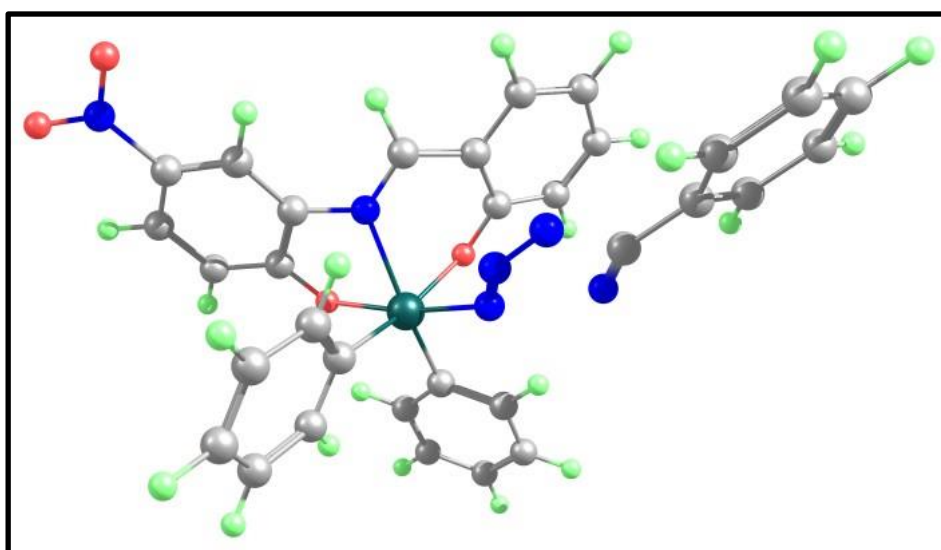


Figure S51. DFT-optimized geometry of Intermediate A and benzonitrile (Transition state 2').

Table S11. Cartesian coordinates of DFT-optimized geometry of Intermediate A and benzonitrile (Transition state 2').

$C_{25}H_{18}N_5O_4Ge + C_7H_5N$

C	3.12932000	0.02583600	-1.04144200
C	2.42672800	-1.17665900	-0.69291000
C	3.09387900	-2.35998800	-0.45860300
C	4.48691400	-2.38160400	-0.58373000
C	5.20282500	-1.23060500	-0.94038500
C	4.53453300	-0.04410300	-1.16749800
N	5.19702300	-3.61459400	-0.33634200

O	4.54512000	-4.61585900	-0.02009400
O	6.42732300	-3.62097800	-0.45303100
O	2.45132100	1.11629100	-1.22439900
N	1.04505200	-0.96171000	-0.67687100
H	2.57339700	-3.26419900	-0.17498300
H	6.27887800	-1.29191000	-1.02260000
H	5.07133800	0.85805500	-1.43191900
Ge	0.66366300	1.08814400	-0.22674100
C	0.14075100	-1.84165400	-0.98103400
H	-2.00656900	-3.42549900	-1.10468600
C	-2.18478400	-2.44029500	-1.52349400
C	-3.38717900	-2.14791900	-2.12512400
H	-4.17765100	-2.88660200	-2.16906600
C	-3.57605200	-0.86825500	-2.68480700
H	-4.51959000	-0.63301600	-3.16631800
C	-2.59967300	0.09925200	-2.60575500
H	-2.75402000	1.09692200	-2.99595400
C	-1.37849100	-0.14641900	-1.92899200
C	-1.16372500	-1.47007300	-1.41776400
O	-0.49778200	0.80787600	-1.83509200
H	0.41099800	-2.90020300	-1.01814100
H	-1.69416900	2.93091200	0.23892900
C	-0.89497300	3.57579400	-0.10496400
C	0.34725100	3.02638500	-0.44426600
C	1.34951700	3.87555100	-0.92583100
H	2.30610600	3.45828300	-1.21392500
C	1.12397200	5.24740300	-1.04954900
H	1.91271200	5.89187000	-1.42508800
C	-0.11047800	5.78774400	-0.69600100
H	-0.28760000	6.85432700	-0.79054900

C	-1.11917900	4.94650800	-0.22747100
H	-2.08818100	5.35624600	0.03913900
C	1.69543000	0.91325500	1.49905400
C	1.71161000	-0.24332300	2.28294700
H	1.12313500	-1.10396100	1.98810900
C	2.46614100	-0.31437600	3.45229900
H	2.46617400	-1.22678300	4.03955900
C	3.21966000	0.78317700	3.86514100
H	3.80891300	0.73104200	4.77455100
C	3.20712100	1.94741200	3.10034900
H	3.78527400	2.81080700	3.41411200
C	2.45335400	2.00749300	1.92781800
H	2.45629100	2.92161800	1.34599600
N	-3.18383300	0.92368200	0.34208500
N	-1.08502000	0.65421500	0.85988700
N	-1.34608100	-0.36532900	1.44718300
C	-5.03368600	-1.89519200	1.82116700
C	-6.25366600	-2.56657400	1.85133300
C	-7.29567000	-2.17614700	1.01241900
C	-7.11306000	-1.10141800	0.14100100
C	-5.89953200	-0.42485200	0.11151100
C	-4.84657400	-0.81661300	0.95134800
H	-4.21484300	-2.20004600	2.45698500
H	-6.38851100	-3.40138600	2.53047500
H	-8.24247000	-2.70466500	1.03554200
H	-7.91781500	-0.79241400	-0.51729000
H	-5.73947200	0.40634500	-0.56312400
C	-3.58074100	-0.08670800	0.86355400
N	-2.30094800	-1.03958200	1.73048100

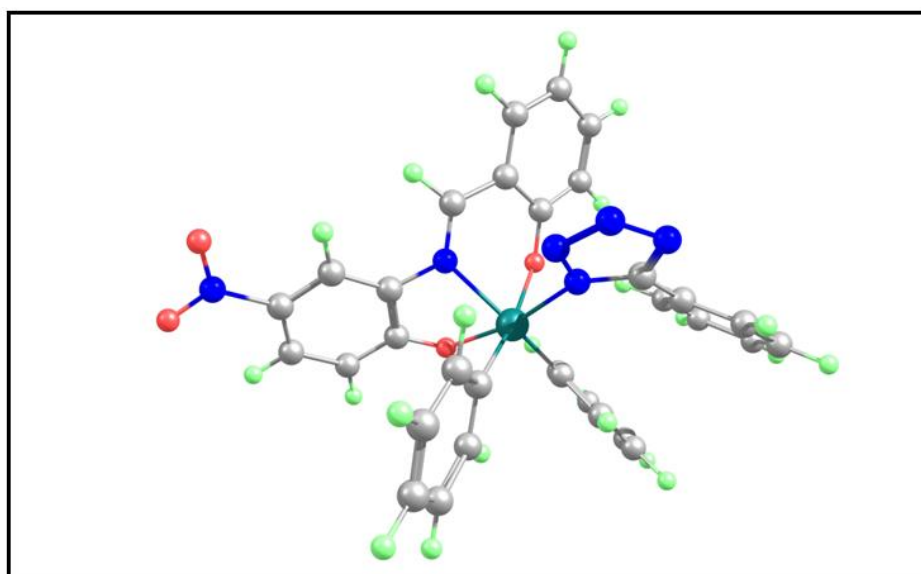


Figure S52. DFT-optimized geometry of Str A and benzonitrile (Intermediate B).

Table S12. Cartesian coordinates of DFT-optimized geometry of Str A and benzonitrile (Intermediate B).

C₃₂H₂₃N₆O₄Ge

C	-2.48345900	-0.63625200	-1.41922700
C	-2.69193700	0.47727500	-0.53701200
C	-3.94795500	0.84337500	-0.10933100
C	-5.04957800	0.11594400	-0.57482300
C	-4.88763100	-0.96408100	-1.45425500
C	-3.62564000	-1.33576400	-1.87181100
N	-6.37377300	0.48626500	-0.13724500
O	-6.49270800	1.44588800	0.63278200
O	-7.33752600	-0.16755000	-0.55216800
O	-1.27068400	-0.94679400	-1.74842200
N	-1.47571200	1.11439200	-0.25065000
H	-4.10251700	1.66446500	0.57692600
H	-5.76647600	-1.49993200	-1.78452700
H	-3.48141900	-2.17665600	-2.53818900
Ge	0.06666800	-0.32599200	-0.28120000

C	-1.32820100	2.39296300	-0.12805200
H	-0.71519000	4.87875600	0.58102800
C	0.07395200	4.40397300	0.00676600
C	1.19683900	5.11744500	-0.35543500
H	1.31372500	6.15263900	-0.05970700
C	2.18415100	4.47939400	-1.12664500
H	3.06762900	5.03219100	-1.42883100
C	2.05523300	3.15730500	-1.50318900
H	2.81884600	2.66971300	-2.09571100
C	0.94266600	2.38079800	-1.09726200
C	-0.07672700	3.04696900	-0.34143600
O	0.87422900	1.12375800	-1.45123100
H	-2.21106200	3.01875300	0.02184900
H	1.89248700	-2.38147800	0.97587100
C	2.10936200	-2.42554300	-0.08572800
C	1.42880000	-1.58423000	-0.96845600
C	1.72038200	-1.66460200	-2.33200400
H	1.19508200	-1.01951400	-3.02525400
C	2.68694200	-2.55267200	-2.80003500
H	2.90728500	-2.60222200	-3.86174800
C	3.37575500	-3.37265000	-1.90645600
H	4.13838500	-4.05422500	-2.26838100
C	3.08253800	-3.30977400	-0.54631300
H	3.61918800	-3.93721600	0.15690900
C	-0.94410200	-1.48381100	1.02575800
C	-1.54344900	-1.03635300	2.20730300
H	-1.43607300	-0.00045000	2.49900900
C	-2.26788400	-1.90833100	3.02031100
H	-2.72671200	-1.53617900	3.93053000
C	-2.40700000	-3.24824900	2.66612700

H	-2.97273100	-3.92579800	3.29714000
C	-1.81881800	-3.70890500	1.48952500
H	-1.92510300	-4.74896800	1.19792500
C	-1.10075100	-2.83163700	0.67895200
H	-0.66728000	-3.20001000	-0.24341400
N	1.14407100	0.64510700	1.22908600
N	0.41679000	1.29946000	2.16642700
N	1.22693400	1.77367900	3.06069200
C	4.67900800	-0.25057700	1.77275600
C	5.84350700	-0.75602300	1.20375000
C	5.99642800	-0.77098700	-0.18201900
C	4.97927000	-0.27039200	-0.99136600
C	3.81419400	0.23564000	-0.42595900
C	3.64768500	0.24094800	0.96198300
H	4.54954900	-0.23247800	2.84743000
H	6.62935500	-1.14412700	1.84279100
H	6.89864600	-1.17653600	-0.62701000
H	5.07979400	-0.29157500	-2.07013000
H	3.01933800	0.59859800	-1.05814900
C	2.43934900	0.76620600	1.61266900
N	2.49852000	1.45497600	2.75309600

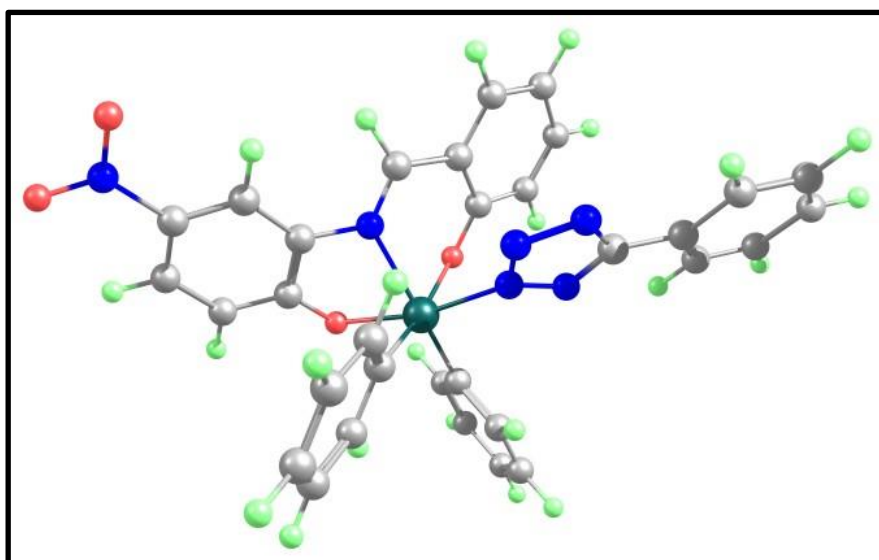


Figure S53. DFT-optimized geometry of Intermediate A and benzonitrile (Intermediate B').

Table S13. Cartesian coordinates of DFT-optimized geometry of Intermediate A and benzonitrile (Intermediate B').

C₃₂H₂₃N₆O₄Ge

C	3.04204300	-0.35103900	1.10539000
C	2.69301000	0.91583400	0.52419500
C	3.65246000	1.81401300	0.11265000
C	5.00053700	1.48198500	0.28936200
C	5.37824100	0.26316700	0.87009400
C	4.41527000	-0.64003200	1.27308400
N	6.01698800	2.41312600	-0.13789500
O	5.66038100	3.48331600	-0.64354200
O	7.20397200	2.10634900	0.02125200
O	2.09307200	-1.16655300	1.44379500
N	1.30282200	1.08497200	0.49958200
H	3.39270400	2.75776500	-0.34650900
H	6.43116000	0.04629200	0.98343400
H	4.68863500	-1.59180400	1.71051000
Ge	0.39271500	-0.81959600	0.33896800
C	0.67980700	2.20582700	0.68362200

H	-0.96462200	4.30831000	0.57149800
C	-1.39679600	3.46565300	1.10196000
C	-2.63749900	3.57630500	1.69052500
H	-3.20154400	4.49825700	1.62113700
C	-3.16393600	2.46953800	2.38508600
H	-4.14336000	2.54606300	2.84577500
C	-2.46755800	1.28320400	2.47314800
H	-2.87740900	0.42015400	2.98248700
C	-1.21320600	1.11921300	1.83473000
C	-0.66952100	2.25785200	1.14880500
O	-0.60080800	-0.02783800	1.90560500
H	1.22999800	3.14611100	0.59610500
H	-1.15367600	-2.91715600	-1.18845100
C	-1.06678500	-3.30959800	-0.18134300
C	-0.40914600	-2.56378200	0.79880300
C	-0.31003200	-3.08878000	2.08949700
H	0.19676200	-2.51733200	2.85734300
C	-0.85632000	-4.33474400	2.39409600
H	-0.77027700	-4.73160000	3.40074100
C	-1.51446900	-5.07054200	1.40870400
H	-1.94256800	-6.03925600	1.64523700
C	-1.61997000	-4.55405400	0.11846700
H	-2.13317200	-5.11823100	-0.65352500
C	1.45699100	-1.22818800	-1.31750200
C	1.66074600	-0.33601200	-2.37460000
H	1.18528600	0.63582900	-2.35340900
C	2.45258600	-0.68763500	-3.46771300
H	2.60031500	0.02218500	-4.27520200
C	3.05484900	-1.94288200	-3.52354600
H	3.67347300	-2.21557400	-4.37226300

C	2.85964100	-2.84377800	-2.47800600
H	3.32592400	-3.82344700	-2.50905300
C	2.07114600	-2.48409700	-1.38613300
H	1.93971900	-3.18805400	-0.57199000
N	-2.46709000	-0.26818800	-0.43260600
N	-1.19988900	-0.03289200	-0.76084900
N	-1.10193900	0.94807400	-1.65541800
C	-5.25015200	1.67990700	-1.95615800
C	-6.63112000	1.83657300	-1.88828300
C	-7.38256500	1.08151300	-0.98794500
C	-6.73962900	0.16668500	-0.15334800
C	-5.35947800	0.00753300	-0.21618300
C	-4.60100400	0.76256600	-1.12065600
H	-4.65670300	2.26374000	-2.64844700
H	-7.12306200	2.55082500	-2.53976900
H	-8.45877200	1.20521100	-0.93636100
H	-7.31619700	-0.42317300	0.55101600
H	-4.84905300	-0.69470000	0.43085000
C	-3.14742400	0.60922300	-1.17048200
N	-2.31913500	1.36289100	-1.93380600

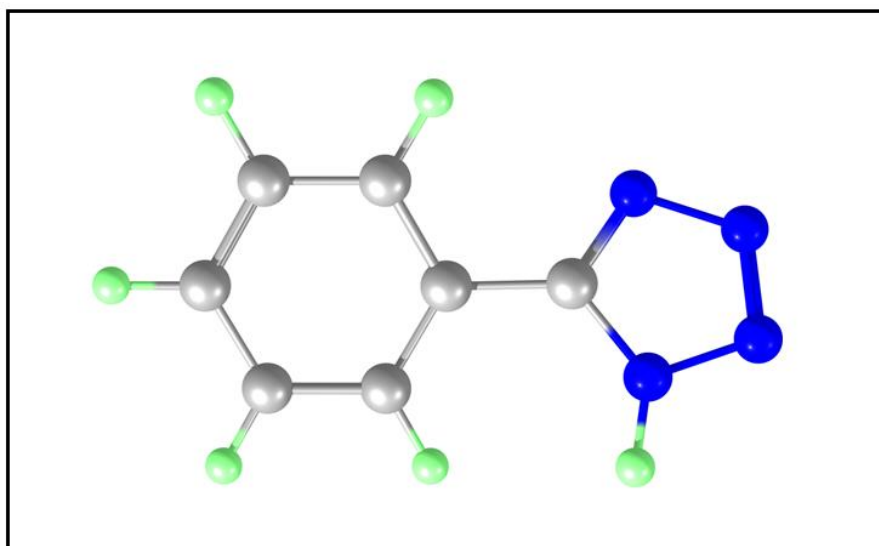


Figure S54. DFT-optimized geometry of 5-substituted 1*H*-tetrazole.

Table S14. Cartesian coordinates of DFT-optimized geometry of 5-substituted 1*H*-tetrazole.

C₇H₆N₄

C	0.42266700	-0.00765200	-0.00739200
C	1.13089800	-1.21344000	0.07478400
C	2.52015100	-1.20452900	0.08299000
C	3.21680300	0.00139400	0.00878800
C	2.51689400	1.20309800	-0.07819900
C	1.12616100	1.20004100	-0.08900100
H	0.57787300	-2.14186100	0.13262100
H	3.06154600	-2.14064600	0.14864600
H	4.30025600	0.00467200	0.01609100
H	3.05301900	2.14214800	-0.14389800
H	0.59767800	2.14283400	-0.17692800
C	-1.03716100	-0.04564200	-0.01063100
N	-1.79644400	-1.11915300	-0.15774400
N	-1.86916000	1.01032400	0.14099100
N	-3.14928400	0.57767600	0.08601800
N	-3.08432700	-0.69637700	-0.09315000
H	-1.67434400	1.98594400	0.30262200

Table S15. Different catalysts used for the synthesis of 5-substituted 1*H*-tetrazoles.

Entry	Catalyst	Catalyst loading (mol %)	Solvent	Temp. (°C)	Time (h)	Yields (%)	Ref.
1	B(C ₆ F ₅) ₃	5	DMF	120	8	94	21
2	InCl ₃	10	DMF	140	24	99	22
3	Mesoporous AlPO ₄	0.1 g	DMF	120	12	92	23
4	Immobilized AlCl ₃ on Al ₂ O ₃	30 mg	DMF	50	1.5-3	83-96	24
5	Bu ₂ Sn(OAc) ₂	1	Benzene	30	60	73-99	25
6	InCl ₃	10	DMF	M.W.	6-12 min	95	26
7	SnCl ₂ -nano-SiO ₂	5	DMF	100	4-6	92	27
8	SnCl ₂	10	DMF	120	6-8	90	27
9	Al(HSO ₄) ₃	10	DMF	120	18	91	28
10	PbCl ₂	10	DMF	120	8-10	81	29
11	Triorganotin alkoxide precatalyst	10	DMF	150	4	93	30
			Bu ₂ O	140		85-99	
12	Sb ₂ O ₃	0.1	DMF	120-130	8	86	31
13	N,N Dimethylpyridin-4-amine (DMPA) based ionic liquids	0.3	Solvent-free	110-115	24	89	32
14	Chitosan supported magnetic ionic liquid nanoparticles (CSMIL)	2.5	Solvent-free	70	1-9	90	33
15	4-(N,N-Dimethylamino)pyridinium acetate	15	Solvent-free	100	2	95	34
16	RuO ₂ /MMT	10	Solvent-free	120	6-8	93	35
17	Tetrabutylammonium fluoride (TBAF)	0.5	Solvent-free	50-120	1-48	97	36
18	[DBU][OAc]	20	Solvent-free	80	1	92	37
19	Expanded perlite	0.05	Solvent-free	110	10 min	95	38
20	Fe ₃ O ₄ @chitin	0.03	Solvent-free	110	20 min	95	39
21	[(C ₆ H ₅) ₂ Ge(L ¹)]	6	Solvent-free	100	8	96	This work
22	[(C ₆ H ₅) ₂ Ge(L ²)]	6	Solvent-free	100	8	90	
23	[(C ₆ H ₅) ₂ Ge(L ³)]	6	Solvent-free	100	8	85	

References

1. V. Rama, K. Kanagaraj and K. Pitchumani, *J. Org. Chem.*, 2011, **76**, 9090-9095.
2. T. Wang, L. Xu and J. Dong, *Org. Lett.*, 2023, **25**, 6222-6227.
3. B. Agrahari, S. Layek, R. Ganguly and D. D. Pathak, *New J. Chem.*, 2018, **42**, 13754-13762.
4. J.-M. Chrétien, G. Kerric, F. Zammattio, N. Galland, M. Paris, J.-P. Quintard and E. Le Grogneq, *Adv. Synth. Catal.*, 2019, **361**, 747-757.
5. R. A. Saikia, A. Dutta, B. Sarma and A. J. Thakur, *J. Org. Chem.*, 2022, **87**, 9782-9796.
6. M. J. Frisch, G. W. Trucks, H. B. Schlegel, G. E. Scuseria, M. A. Robb, J. R. Cheeseman, G. Scalmani, V. Barone, B. Mennucci and G. A. Petersson, *Gaussian Inc*, 2009.
7. A. D. Becke, *J. Chem. Phys.*, 1993, **98**, 5648-5652.
8. C. Lee, W. Yang and R. G. Parr, *Phys. Rev. B*, 1988, **37**, 785.
9. S. Grimme, J. Antony, S. Ehrlich and H. Krieg, *J. Chem. Phys.*, 2010, **132**.
10. S. Grimme, S. Ehrlich and L. Goerigk, *J. Comput. Chem.*, 2011, **32**, 1456-1465.
11. A. J. H. Wachters, *J. Chem. Phys.*, 1970, **52**, 1033-1036.
12. P. J. Hay, *J. Chem. Phys.*, 1977, **66**, 4377-4384.
13. M. J. Frisch, J. A. Pople and J. S. Binkley, *J. Chem. Phys.*, 1984, **80**, 3265-3269.
14. T. Clark, J. Chandrasekhar, G. W. Spitznagel and P. V. R. Schleyer, *J. Comput. Chem.*, 1983, **4**, 294-301.
15. K. Fukui, *Acc. Chem. Res.*, 1981, **14**, 363-368.
16. R. F. Ribeiro, A. V. Marenich, C. J. Cramer and D. G. Truhlar, *J. Phys. Chem. B*, 2011, **115**, 14556-14562.
17. G. Luchini, J. V. Alegre-Requena, I. Funes-Ardoiz and R. S. Paton, *F1000Research*, 2020, **9**, 291.
18. A. Moser, K. Range and D. M. York, *J. Phys. Chem. B*, 2010, **114**, 13911-13921.
19. D. McQuarrie, Sausalito, CA, 2000, 222-223.
20. R. Dennington, T. Keith, J. Millam and V. GaussView, Shawnee Mission KS, *GaussView*, Version, 2009, **5**.
21. S. K. Prajapati, A. Nagarsenkar and B. N. Babu, *Tetrahedron Lett.*, 2014, **55**, 3507-3510.
22. H. B. Sun, W. L. Chen, Y. H. Sun, P. Qin and X. Qi, *Adv. Mat. Res.*, 2012, **396-398**, 2416-2419.
23. M. Ai, L. Lang, B. Li and Z. Xu, *Chem. Lett.*, 2012, **41**, 814-816.
24. H. M. Nanjundaswamy and H. Abrahamse, *Heterocycles*, 2014, **89(9)**, 2137-2150.
25. H. Yoneyama, N. Oka, Y. Usami and S. Harusawa, *Tetrahedron Lett.*, 2020, **61**, 151517.
26. V. S. Patil, K. P. Nandre, A. U. Borse and S. V. Bhosale, *E-J. Chem.*, 2012, **9**, 1145-1152.
27. A. Kumar, S. Kumar, Y. Khajuria and S. K. Awasthi, *RSC Adv.*, 2016, **6**, 75227-75233.
28. S. M. Sajadi, M. Khalaj, S. M. H. Jamkarani, M. Mahame and M. Kashef, *Synth. Commun.*, 2011, **41**, 3053-3059.
29. R. Kant, V. Singh and A. Agarwal, *C. R. Chim.*, 2016, **19**, 306-313.
30. J. M. Chrétien, G. Kerric, F. Zammattio, N. Galland, M. Paris, J. P. Quintard and E. Le Grogneq, *Adv. Synth. Catal.*, 2019, **361**, 747-757.
31. G. Venkateshwarlu, K. C. Rajanna and P. K. Saiprakash, *Synth. Commun.*, 2009, **39**, 426-432.
32. S. A. Ghumro, S. Saleem, M. Al-Rashida, N. Iqbal, R. D. Alharthy, S. Ahmed, S. T. Moin and A. Hameed, *RSC Adv.*, 2017, **7**, 34197-34207.
33. A. Khalafi-Nezhad and S. Mohammadi, *RSC Adv.*, 2013, **3**, 4362-4371.
34. N. Nowrouzi, S. Farahi and M. Irajzadeh, *Tetrahedron Lett.*, 2015, **56**, 739-742.
35. H. R. Pawar and R. C. Chikate, *J. Mol. Struct.*, 2021, **1225**, 128985.
36. D. Amantini, R. Beleggia, F. Fringuelli, F. Pizzo and L. Vaccaro, *J. Org. Chem.*, 2004, **69**, 2896-2898.
37. M. A. Siddiqui, M. H. Shaikh, A. A. Nagargoje, T. T. Shaikh, V. M. Khedkar, P. P. Deshpande and B. B. Shingate, *Res. Chem. Intermed.*, 2022, **48**, 5187-5208.
38. R. Jahanshahi and B. Akhlaghinia, *RSC Adv.*, 2015, **5**, 104087-104094.
39. M. Zarghani and B. Akhlaghinia, *RSC Adv.*, 2016, **6**, 31850-31860.